Cassini SAR Imagery of Titan and Related Work

Bryan Stiles
Radar Science and Engineering Section
Jet Propulsion Laboratory,
California Institute of Technology

Acknowledgments

- Far too many people to list have contributed to this work, but here is a brief attempt to summarize.
  - The late **William T. K. Johnson** who successfully shepherded Cassini RADAR from concept to fruition.
  - The team of Italian engineers led by **Enrico Flamini** who built the RF portion of the RADAR instrument
  - The JPL team that built the Digital hardware and integrated the instrument: **Andrew Berkun, Eastwood Im, Joseph Okonek, Kevin Wheeler**, and numerous others.
  - The many excellent JPL engineers who have worked on the RADAR instrument postlaunch team: **Yanhua Anderson, Rudy Boehmer, Anne Bunker, Phil Callahan, Yonggyu Gim, Eric Gudim, Gary Hamilton, Scott Hensley, Kathleen Kelleher, Otfried Liepack, Mahta Moghaddam, Ladislav Roth, Scott Shafer, Joanna Shimada, Lisa Tatge, Chandini Veramacheneni, Richard West.**
  - The PI, **Charles Elachi**, and Science Team Lead, **Stephen Wall**, and the rest of the Cassini RADAR Science Team and associated scientists.
  - The Cassini Project personnel who transported the RADAR to where it could do the most good.

Overview

- Background
  - Cassini radar instrument
  - SAR processing method
- Images of Titan
- Topography from SAR (SARTopo)
- Estimates of Titan’s spin axis and spin rate.
- Conclusions and Future Work.

Background

Cassini Radar Overview

- Ku-band 13.77 GHz radar
- Modes:
  - SAR 935 kHz chirp bandwidth, target=Titan
  - Scatterometer, 117 kHz, target=Titan, icy moons
  - Altimeter, 4.68 MHz, target=Titan
  - Radiometer, source=Saturn, Titan, icy moons, rings, Jupiter

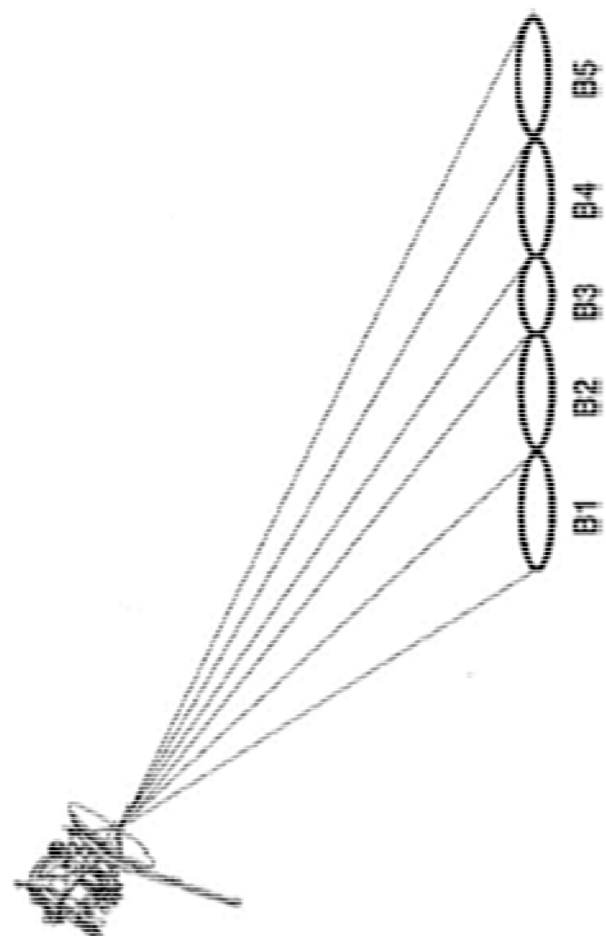

Overview of Cassini Radar Titan Flyby

Radiometry only	Scatterometry	Altimetry SAR
raster scans in two polarizations	raster scan in one polarization	line scan in one polarization
600 km < footprint < 170 km	170 km < footprint < 60 km	60 km < footprint < 5 km

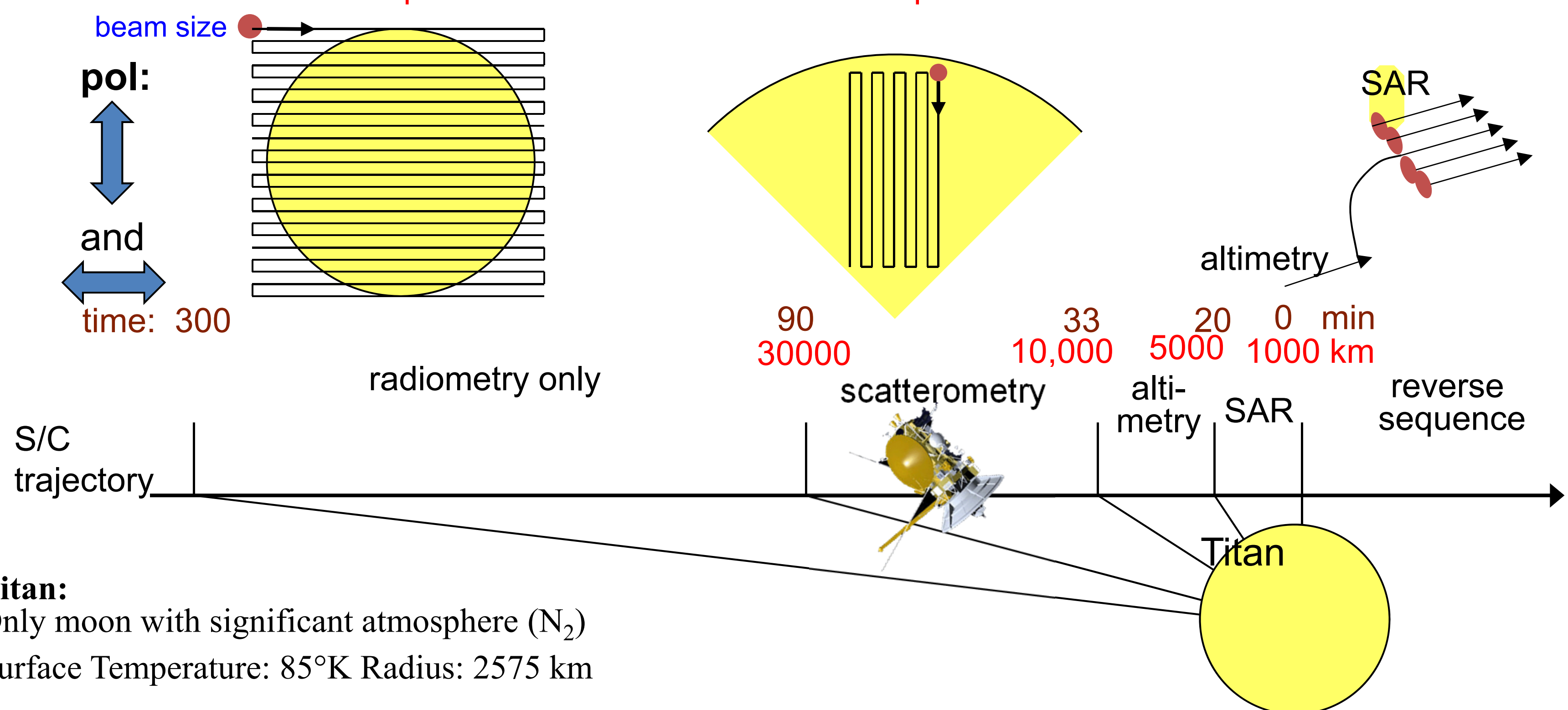

Titan:
Only moon with significant atmosphere (N_2)
Surface Temperature: 85°K Radius: 2575 km

Cassini SAR Characteristics

- Burst Mode SAR (7% burst duty cycle)

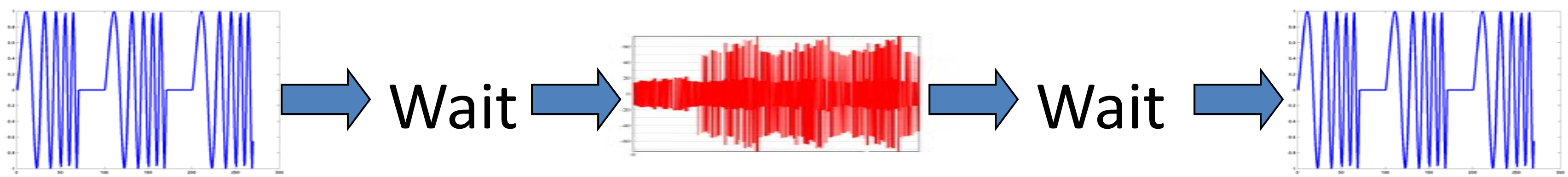

Transmit pulse train | Receive Echo | Repeat

  - Multiple bursts cannot be processed coherently due to large grating lobes.
- Data is compressed using 8 to 2 bit BAQ compression.
- Highly variable viewing geometry
  - Resolution varies from 300 m to 2 km along swath, or 5 km for HISAR.
  - Noise Floor varies from -30 dB to -6 dB.
  - Number of looks varies from 3 at closest approach to 20 or more for HISAR.

SAR Processing Block Diagram

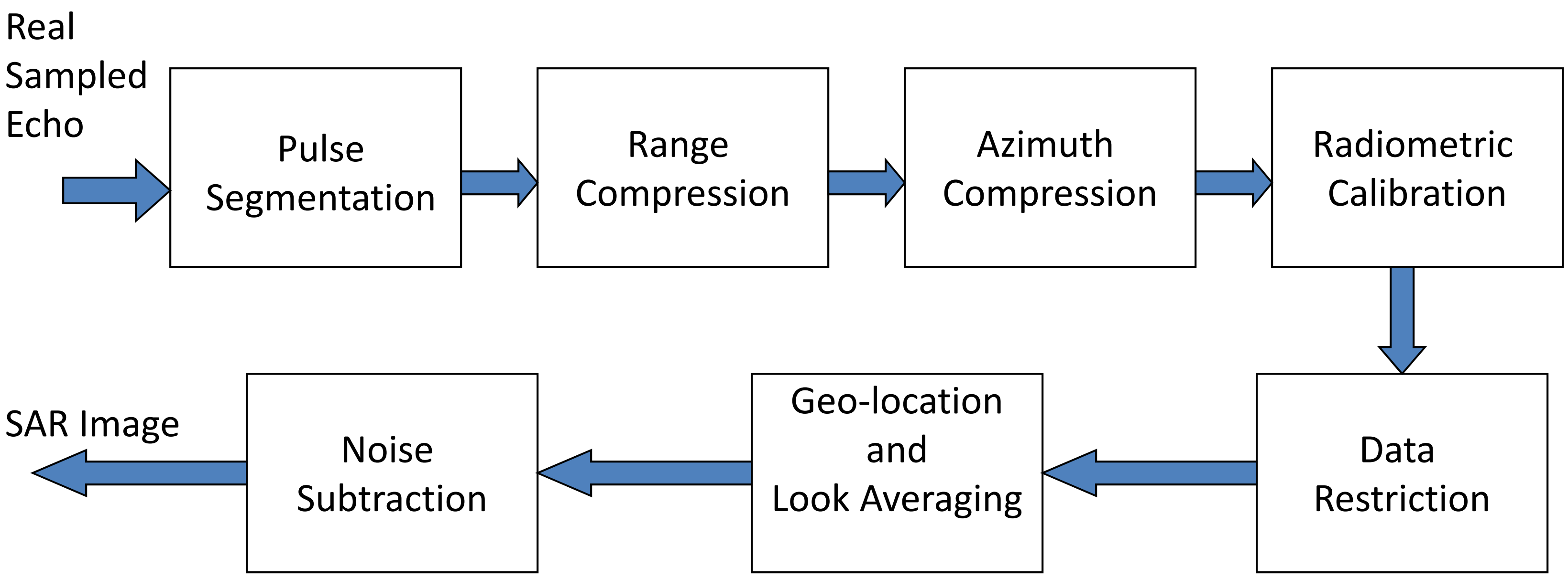

Pulse Segmentation

- Real-Valued samples of video offset data
- Segmented into constant duration overlapping temporal windows
  - Separately range compress each returning pulse.
  - Preserve energy returned simultaneously from consecutive pulses.

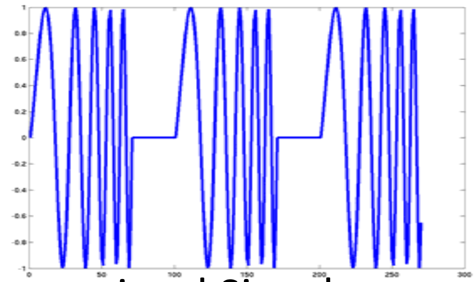
Transmitted Signal

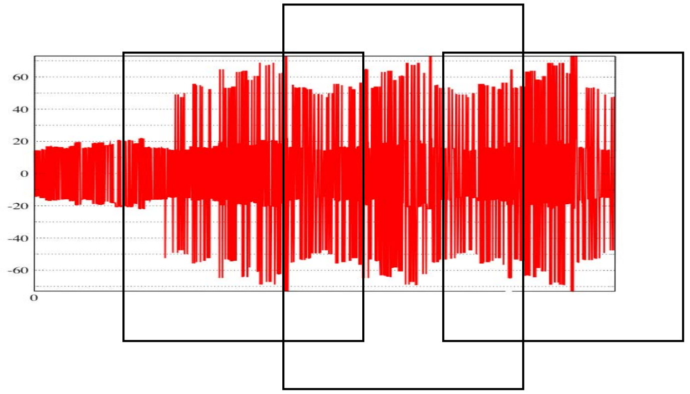

Returned echo with overlapping pulse segmentation

Range Compression

- Each segment convolved with matched filter
  - Estimate of Doppler shifted, base-banded echo from point target at boresight.
  - DC bin zeroed out.
- Output = amplitude M and phase Φ as a function of range r and pulse number.

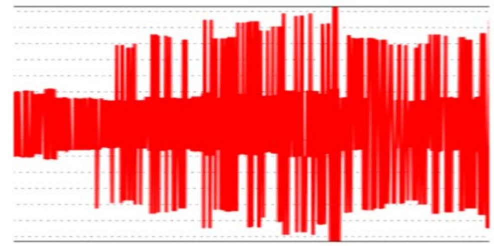

convolved with

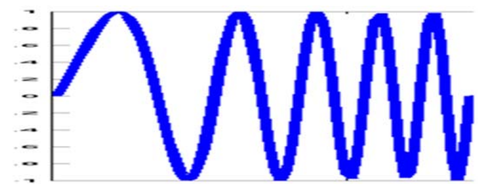

yields

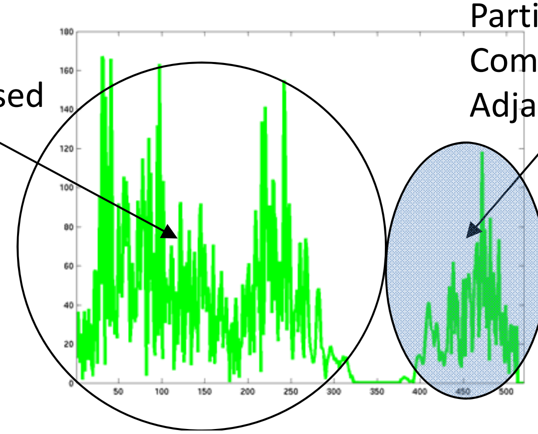

Azimuth Compression

- Input: Each range bin sampled once per pulse
- Convolved with azimuth matched filter
  - Linear FM chirp
  - Center frequency is Doppler centroid as a function of range
  - Chirp rate is derivative of Doppler with time
- Output is $M(r,\Delta f_{dop})$ and $\Phi(r,\Delta f_{dop})$

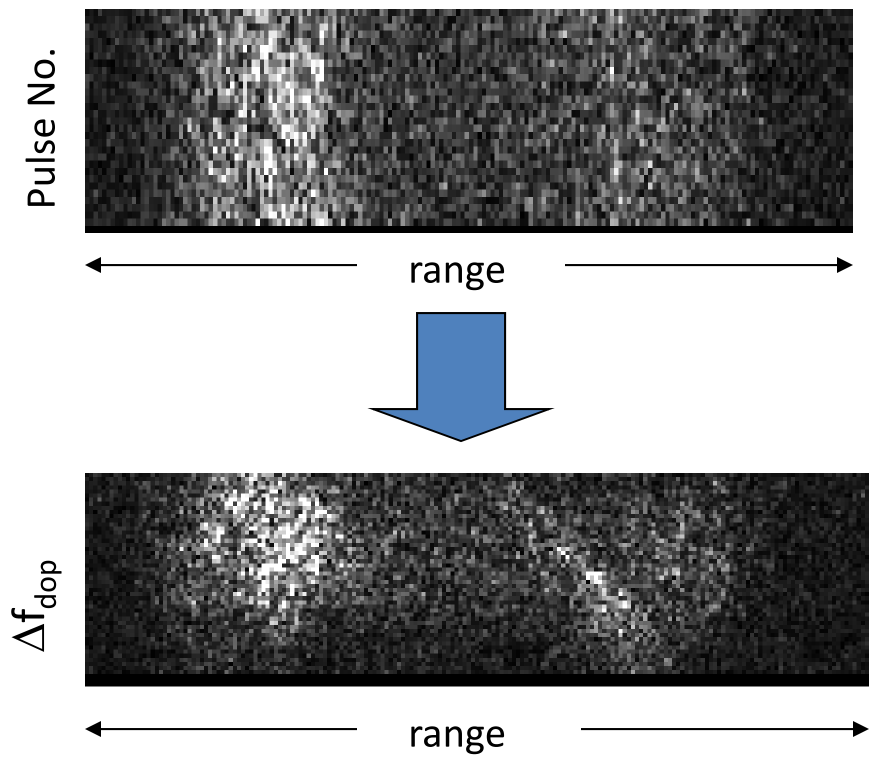

Radiometric Calibration

- Normalize M to account for radar equation. M=M/X

$$X = \sqrt{\frac{P_t \lambda^2 G_a^2 G_l G_c G_r A}{64\pi^3 r^4}}$$

P_t = Transmit Power
λ = Wave length
G_a = antenna gain
G_l = calibrated attenuator gain
G_c = Azimuth and Range compression gain
G_r = calibrated receiver gain
A = pixel area on surface
r = range

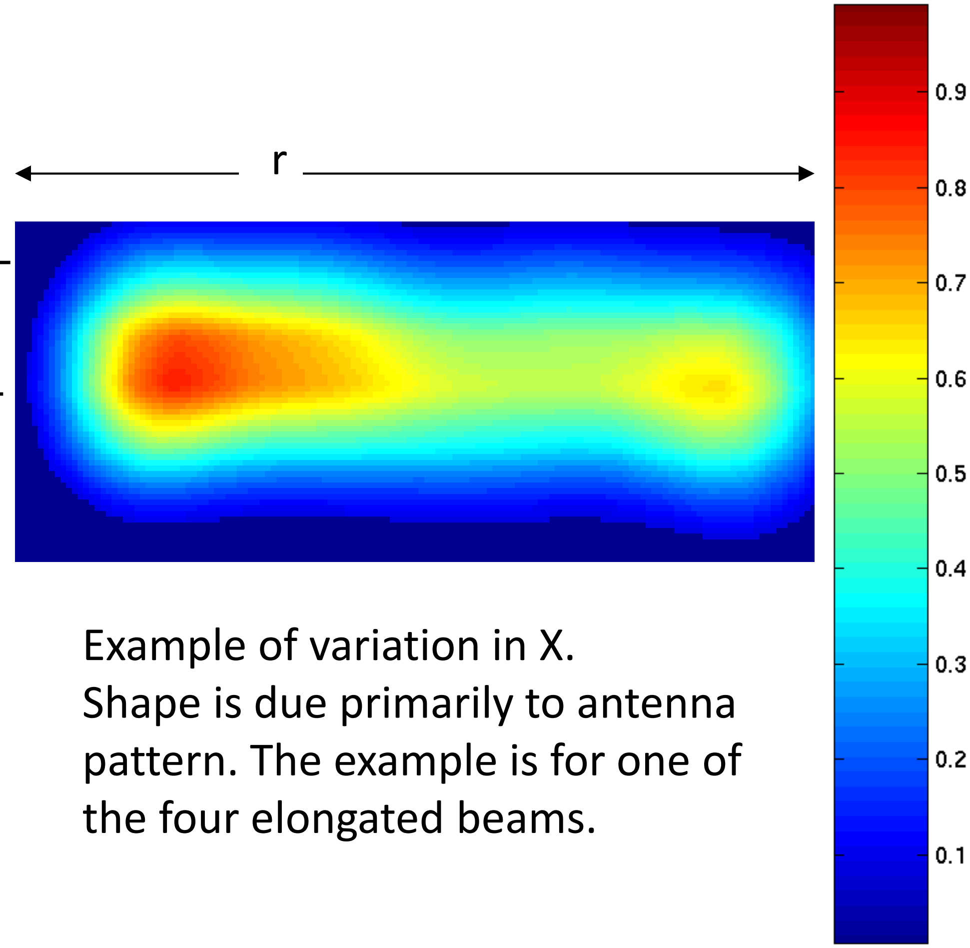

Example of variation in X.
Shape is due primarily to antenna pattern. The example is for one of the four elongated beams.

Data Restriction

- Determine which pixels in range and Doppler space are usable.
  - Two way Antenna Gain within 10 dB of peak gain
  - Signal to Ambiguity ratio > 5 dB
- Usually first criteria is dominant
- Unusual pointing cases can make the second criteria dominant.

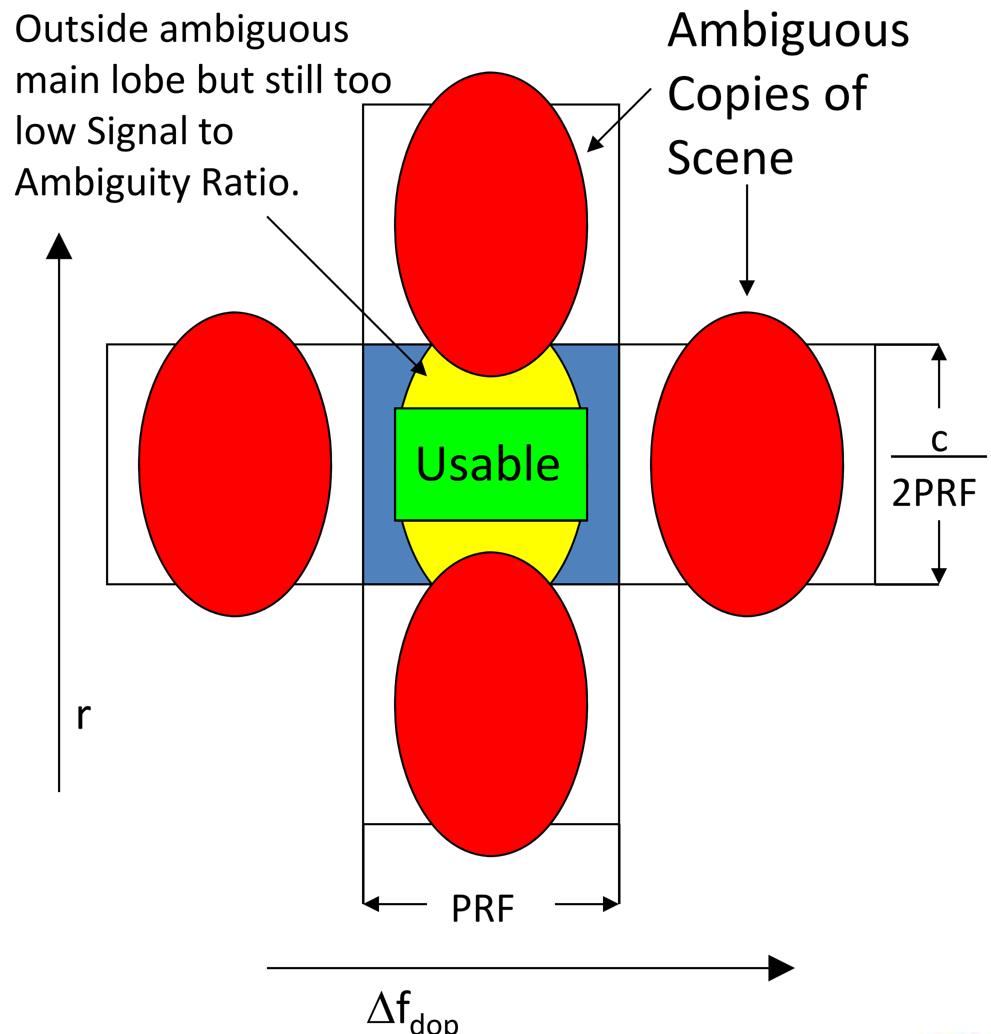

Effect of Ambiguity Restriction

Without Amb. Restrict.

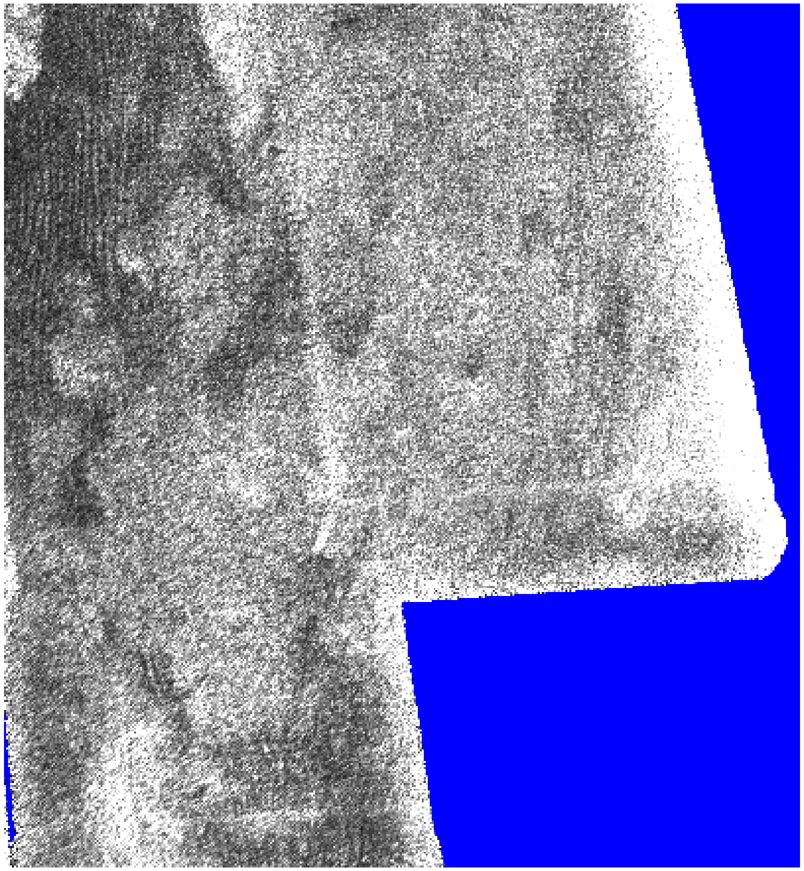

With Amb. Restrict.

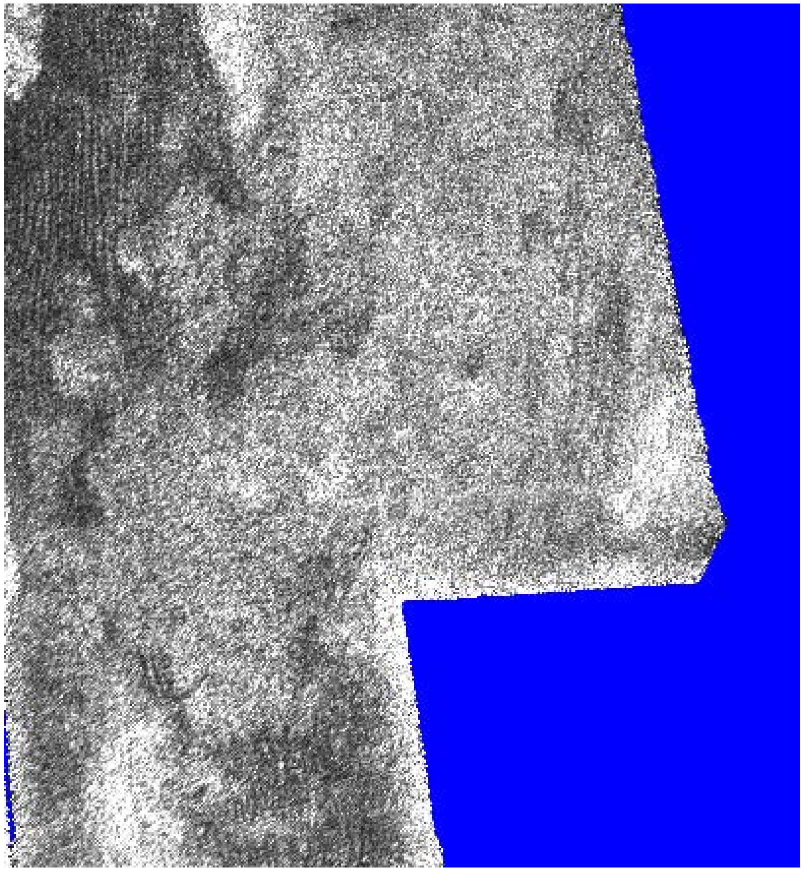

Geo-Location/Multi-Looking

- Usable pixels are interpolated
  - onto an oblique cylindrical surface grid
  - assuming a spherical 2575 km radius Titan
  - with 2-D sinc interpolation
- Multiple antenna footprints contribute to the same surface pixel
  - Detected and averaged incoherently
  - 3-4 looks at closest approach, 20 or more at the highest SAR altitude

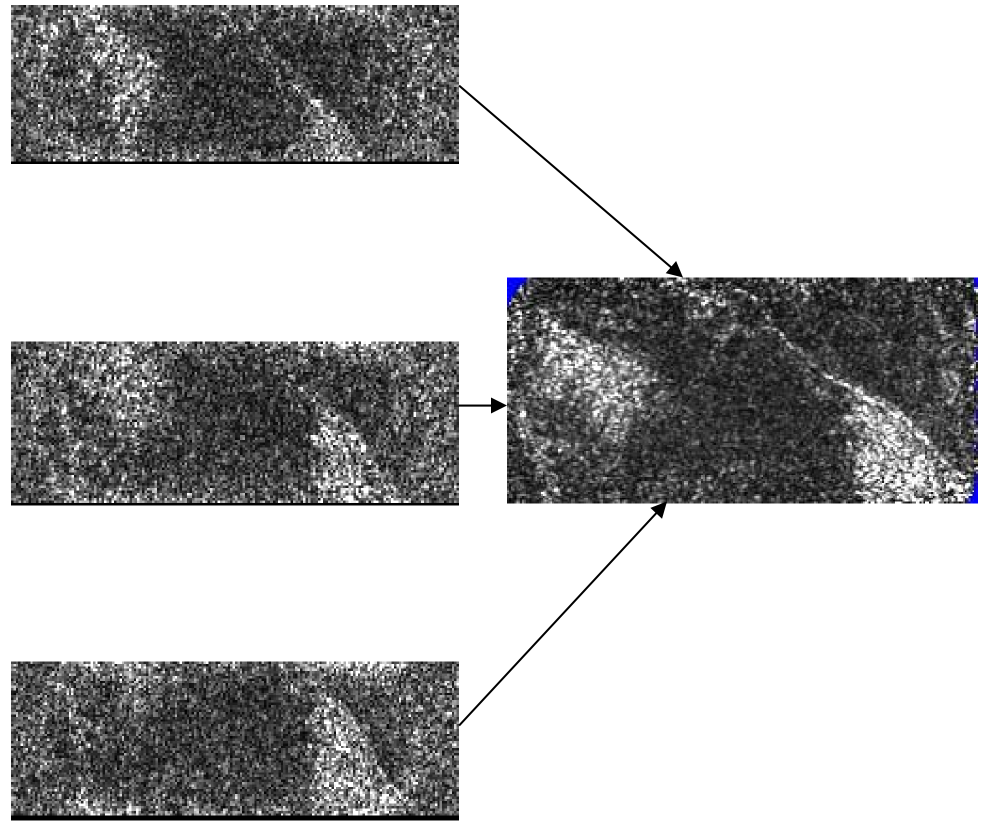

Noise Subtraction

- Noise subtraction performed because:
  - High altitude SAR can have SNR less than 0 dB for radar dark regions
- Simulated noise only data passed through entire SAR processor to estimate noise energy image.
  - Gaussian noise
  - Variance computed from receive only calibration
- Noise image is subtracted from standard image

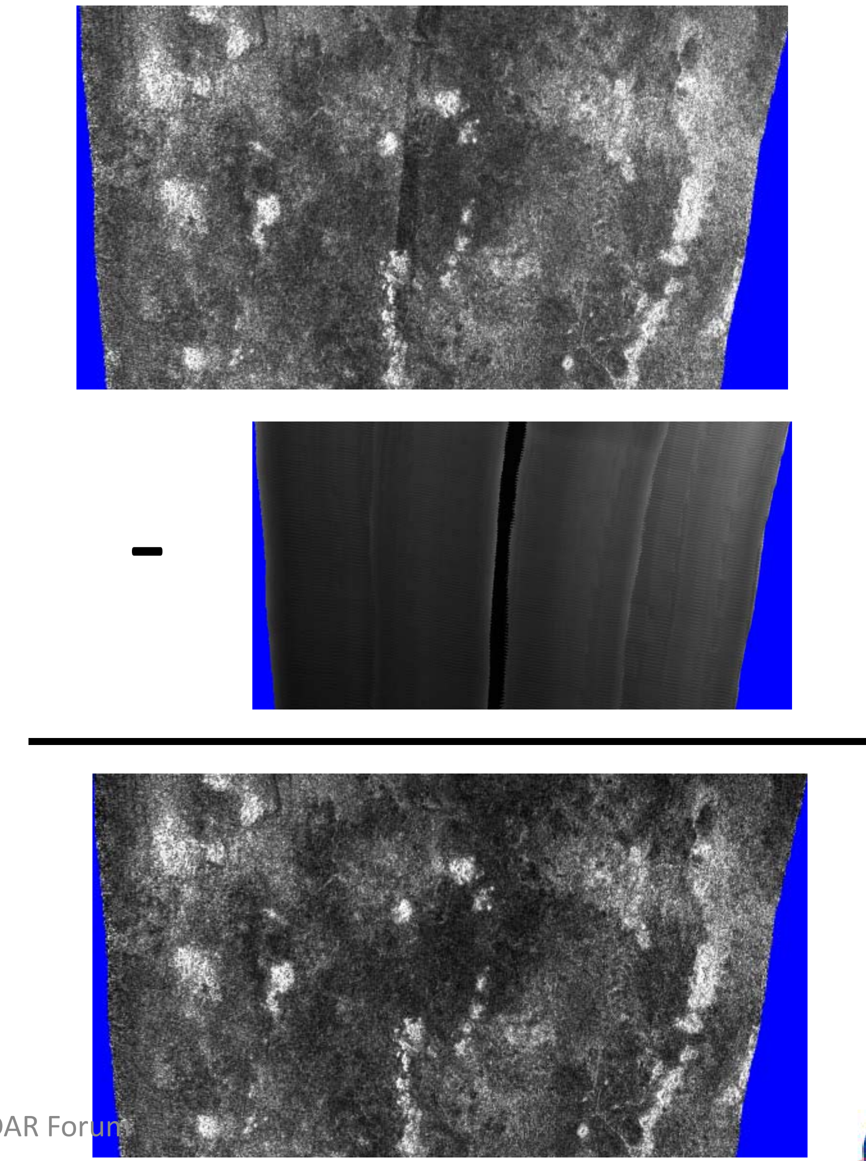

Automated Doppler Range Tracking Method

- Raw SAR image
  - Uncalibrated
  - Range compressed
  - Azimuth compressed
  - Detected
- Correlated with X^2 image
  - Radar equation calibration coefficient
- Peak of correlation yields Doppler and range centroid offsets.
- Offsets are fit to time-varying polynomial.
- SAR processor is rerun with estimated offsets.

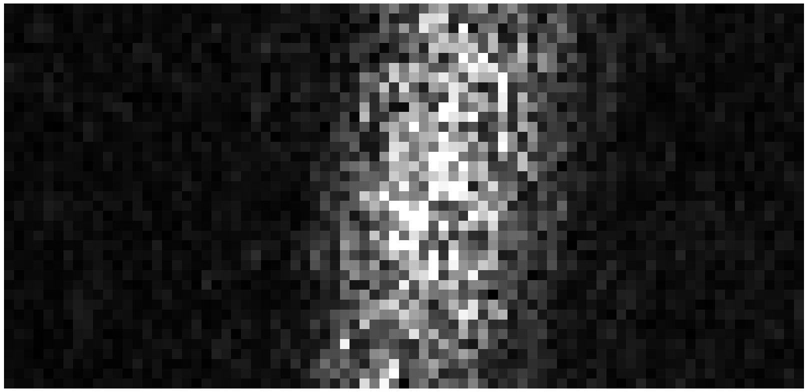

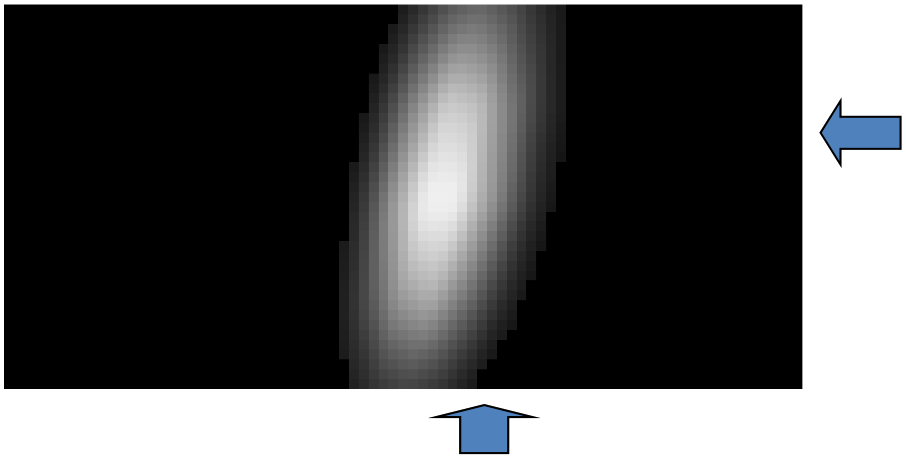

Efficacy of Doppler/Range Tracking using Predicted S/C Ephemeris and Attitude

Before

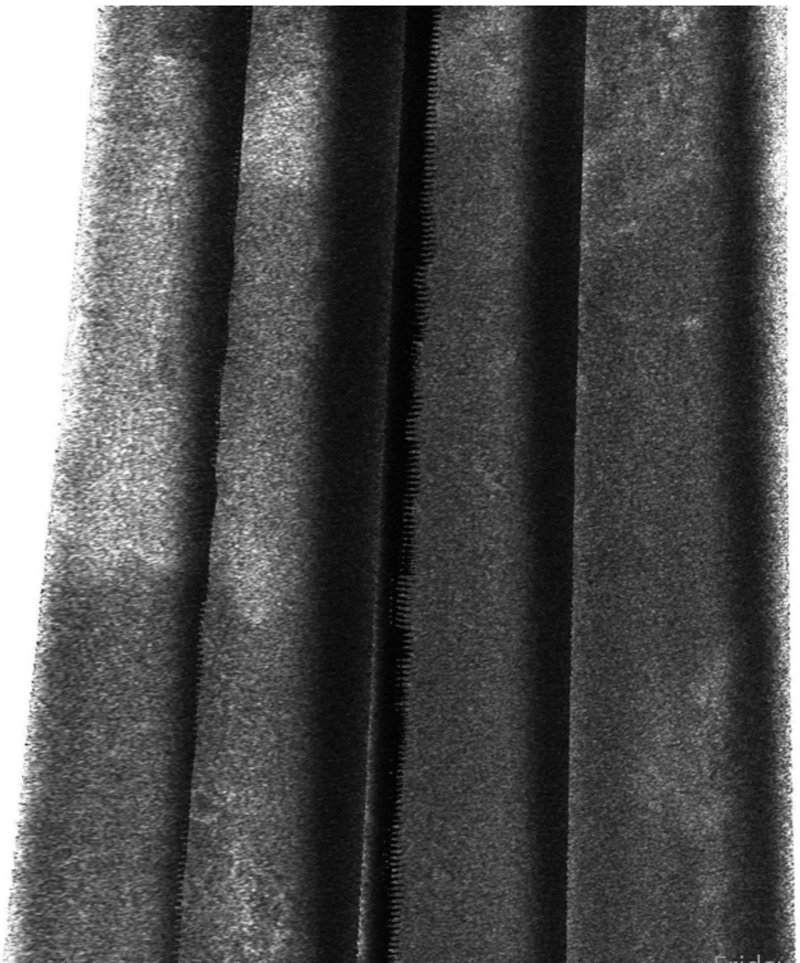

After

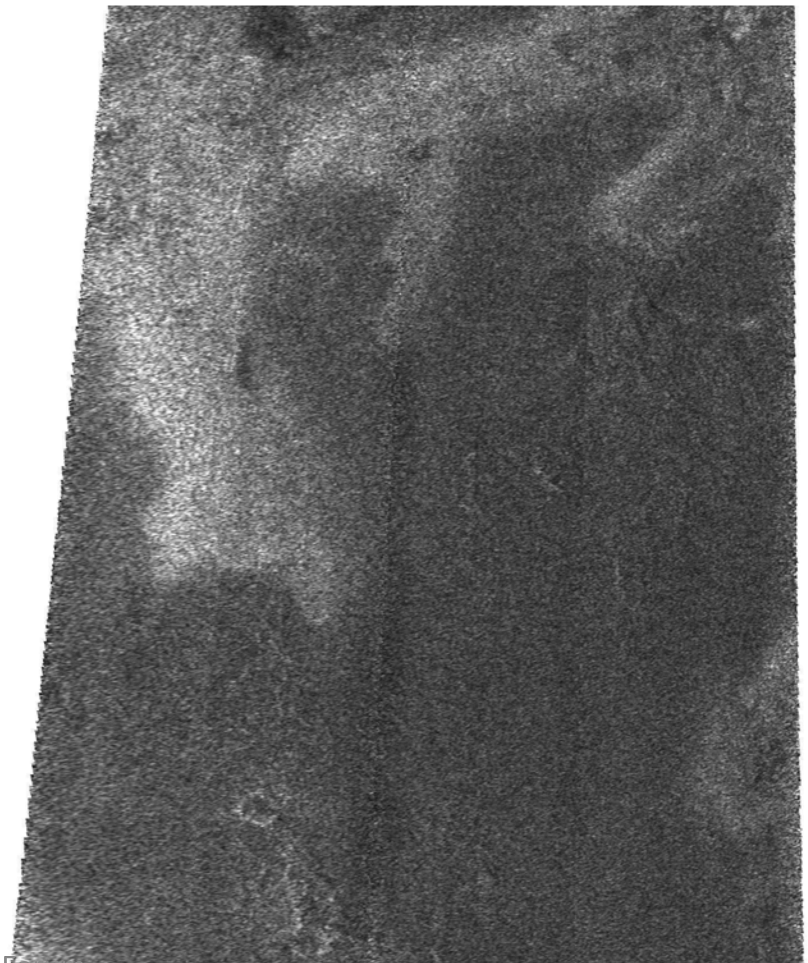

Efficacy of Doppler/Range Tracking using Reconstructed S/C Ephemeris and Attitude

Before

After

SAR Images

North Polar Proj. (60-90 N)

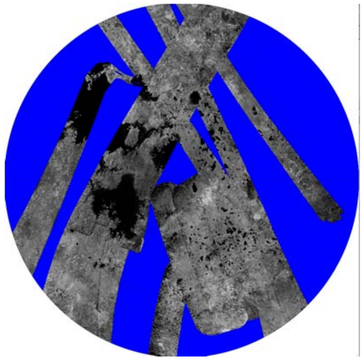

Western Hemisphere

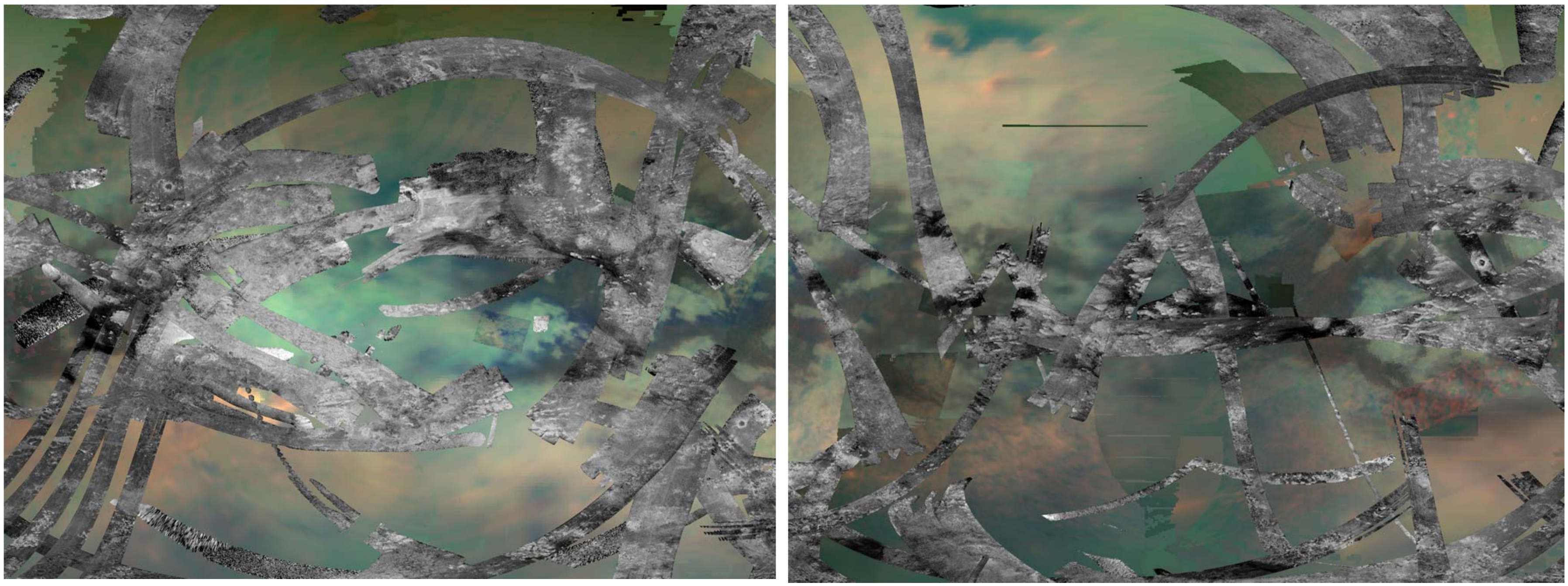

Eastern Hemisphere

South Polar Proj. (60-90 S)

Northern Hemisphere Liquid Methane Lakes

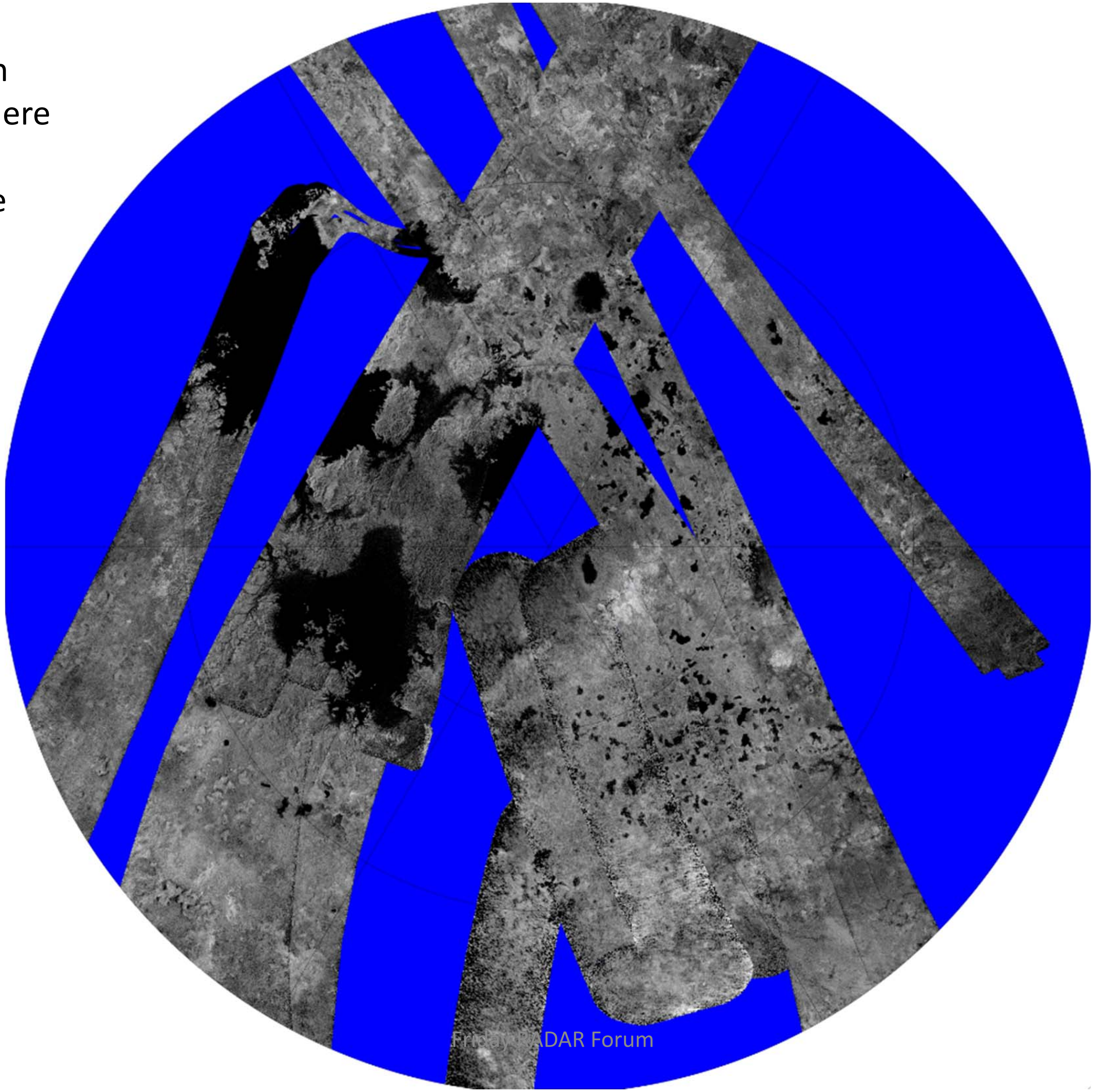

Kraken Mare --- Liquid Methane Sea, Largest Body of Methane on Titan

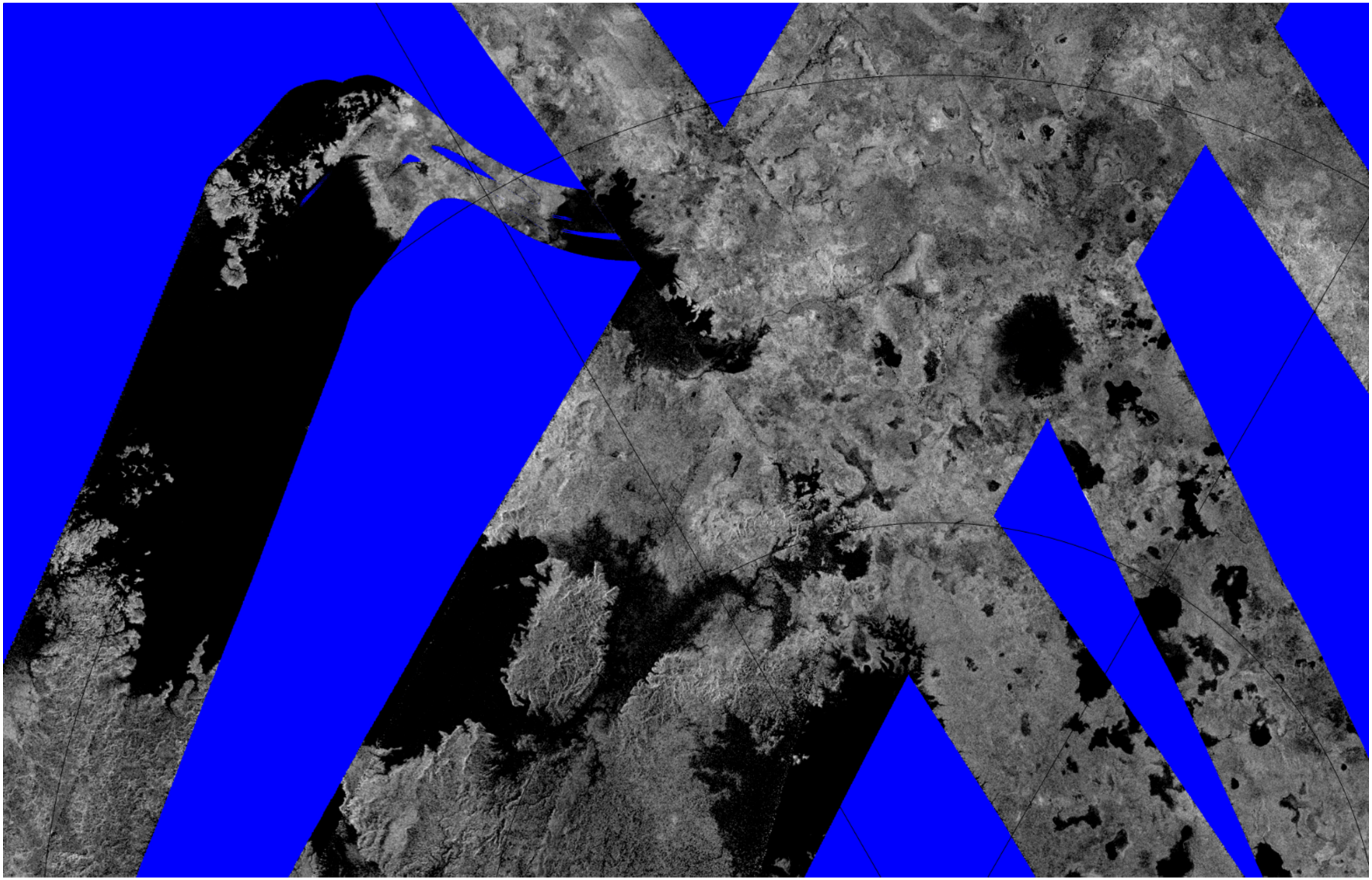

Dry Lakes and Partially filled Basins in Upper Left

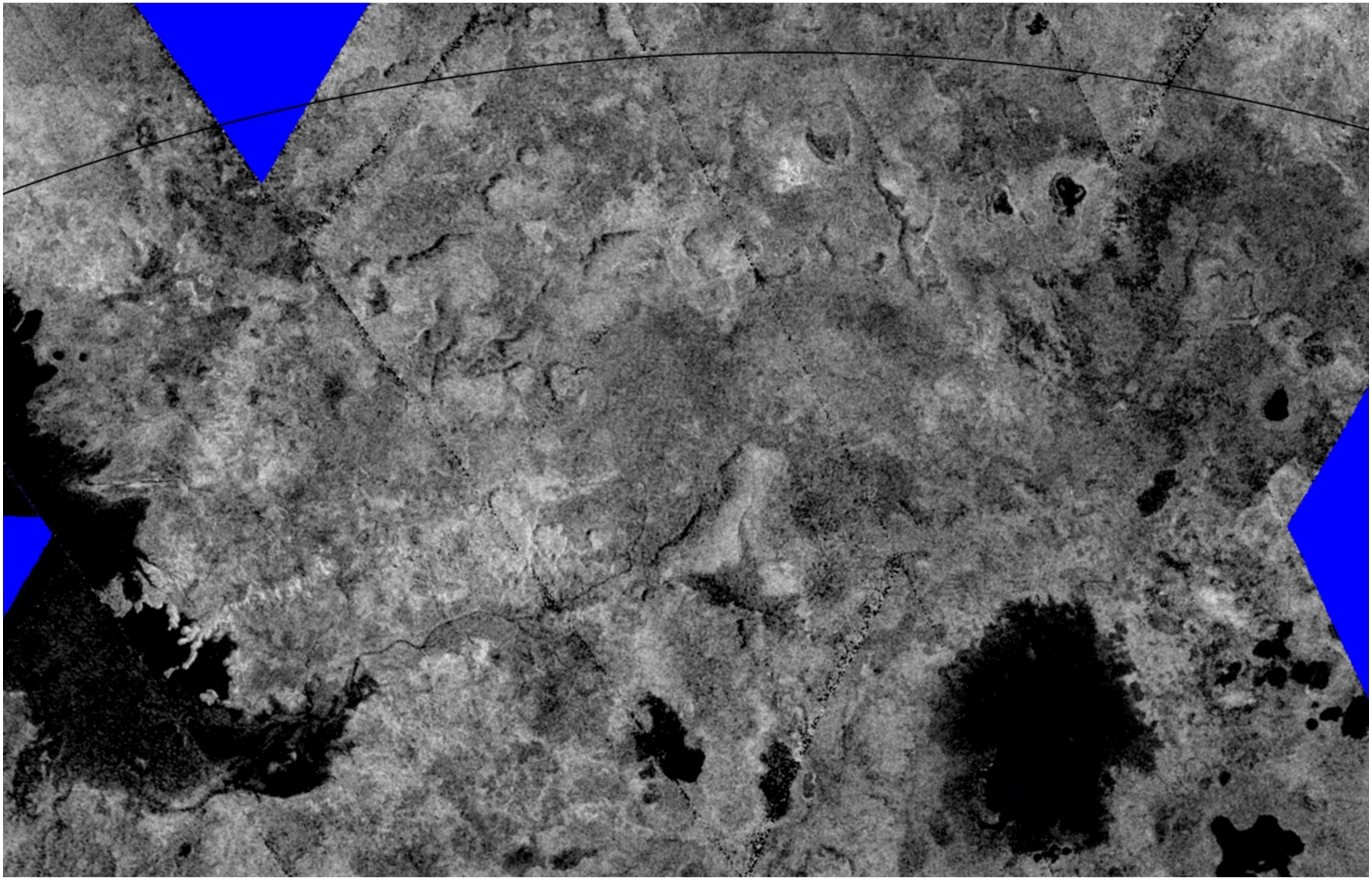

Ligeia Mare, Second Largest Body with channels and nearby dry lake beds.

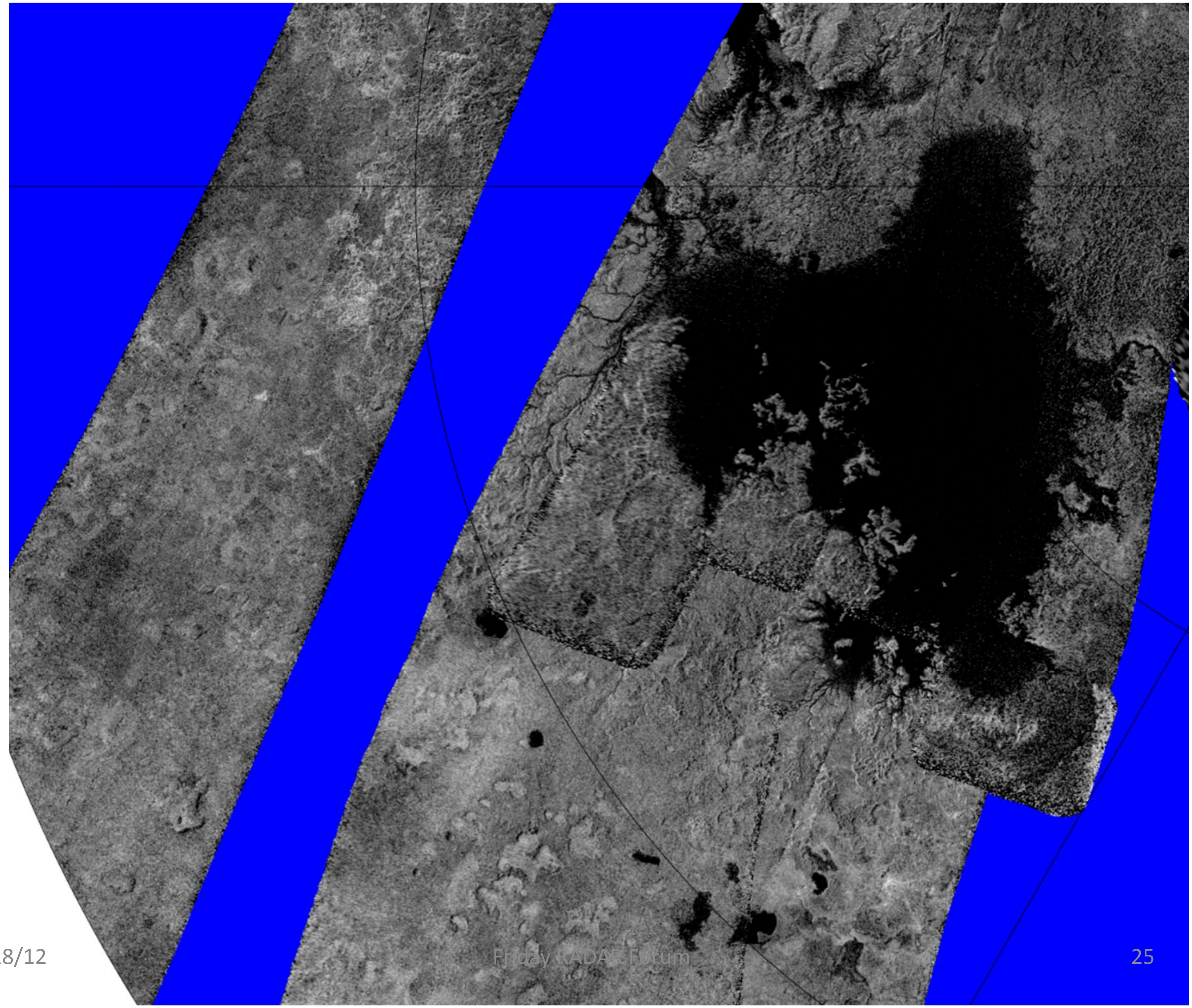

Western hemisphere, 67 S to 67 N

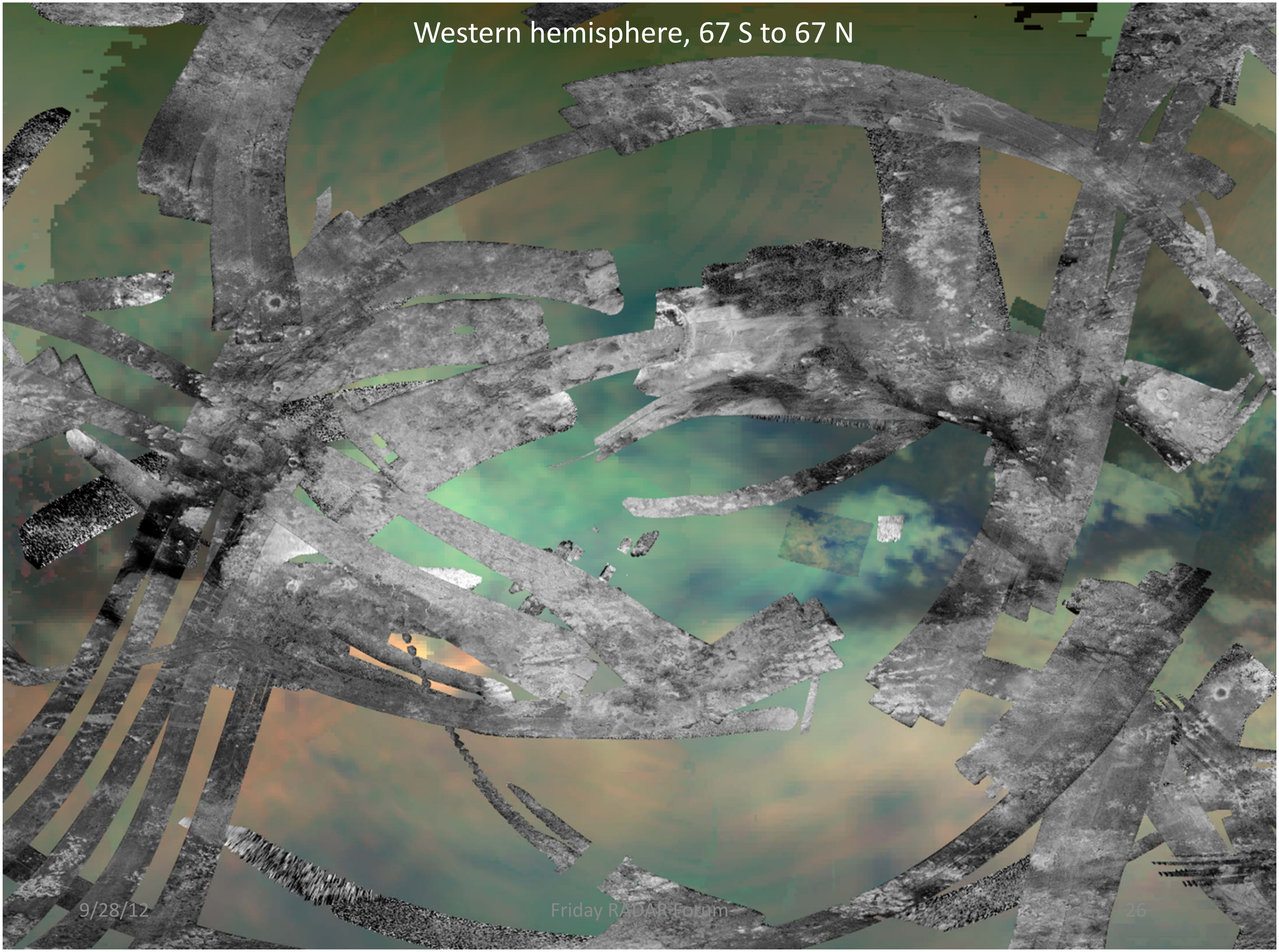

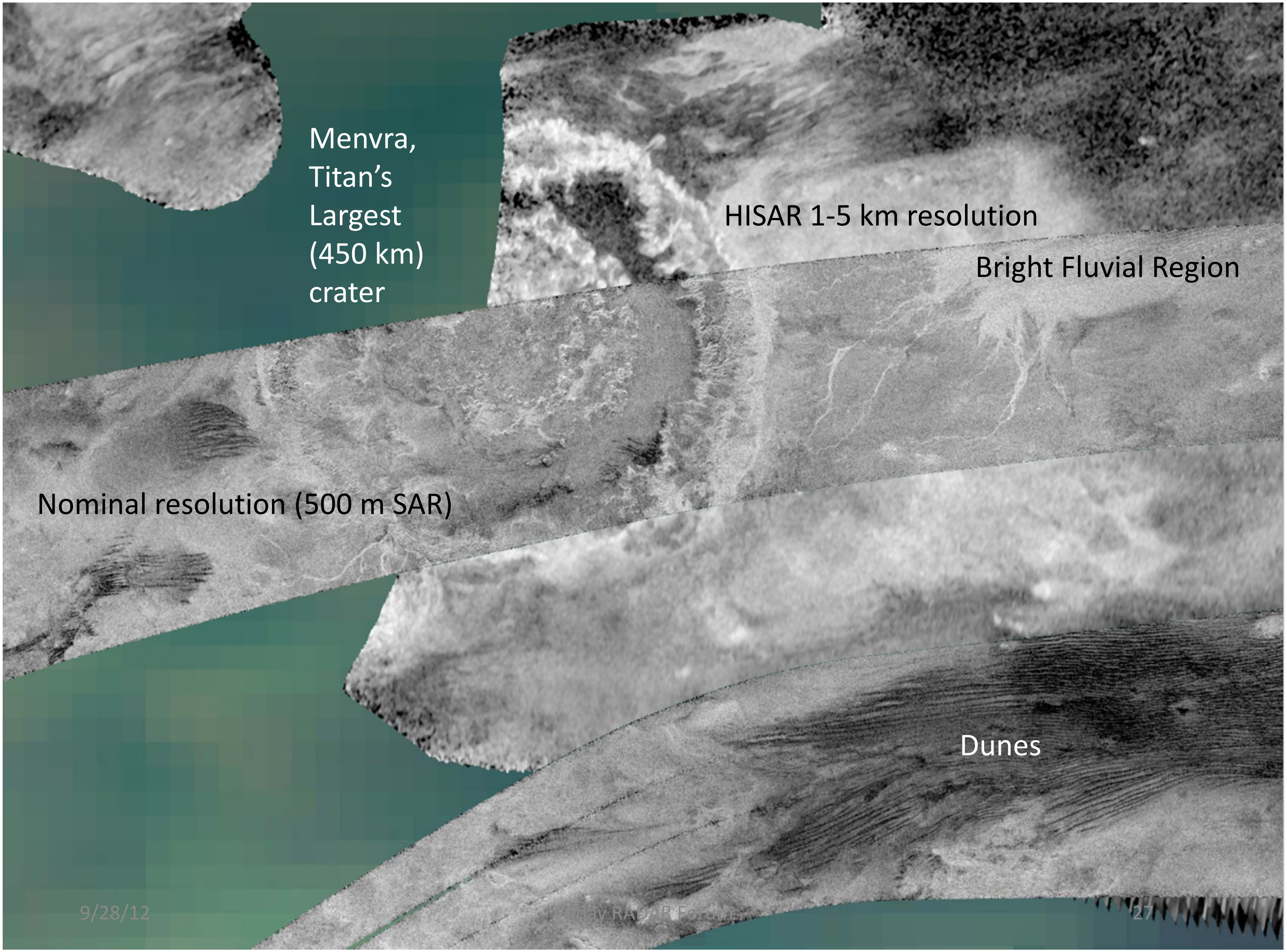
Menvra,
Titan's
Largest
(450 km)
crater
HISAR 1-5 km resolution
Bright Fluvial Region
Nominal resolution (500 m SAR)
Dunes

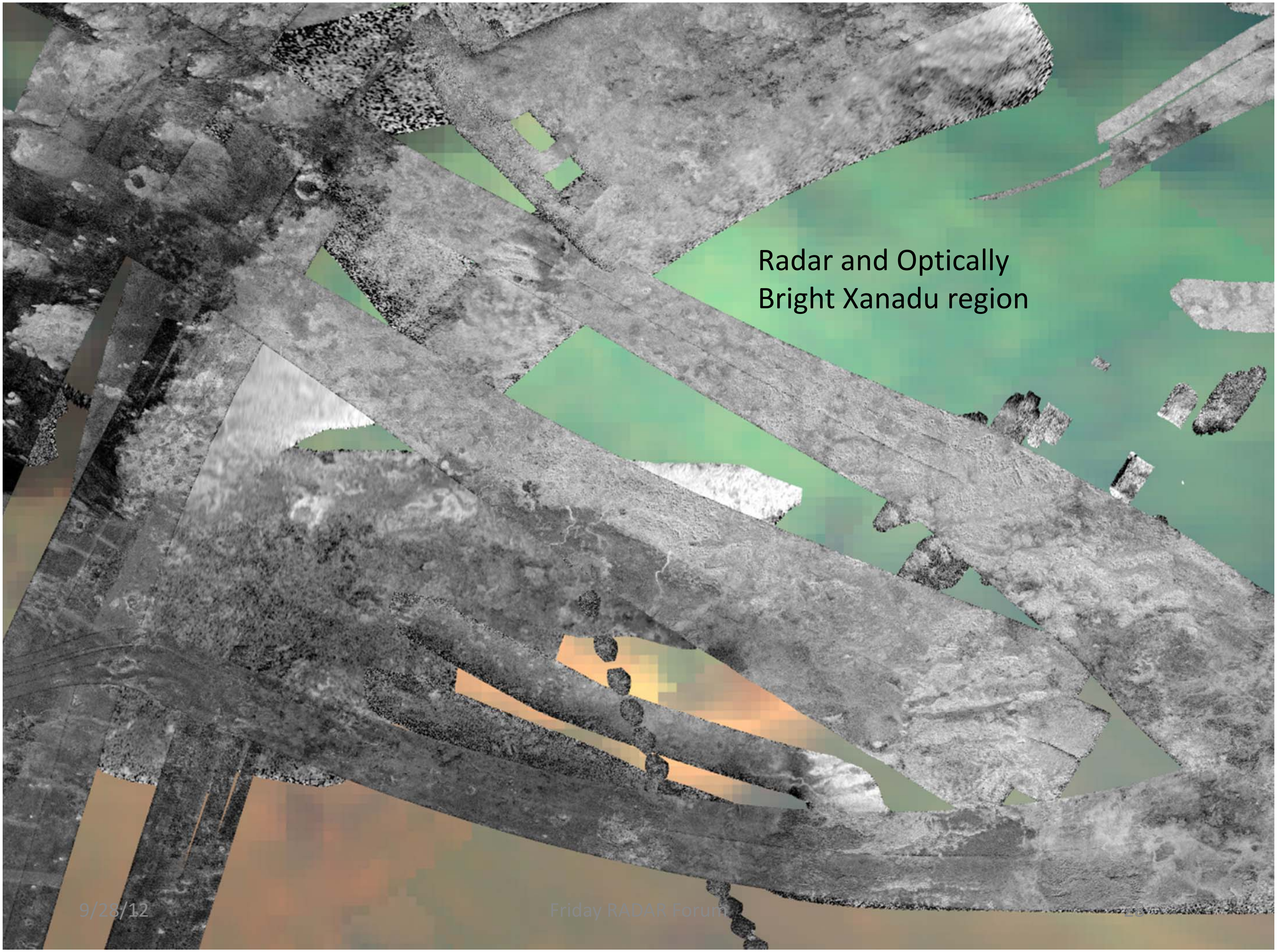
Radar and Optically
Bright Xanadu region

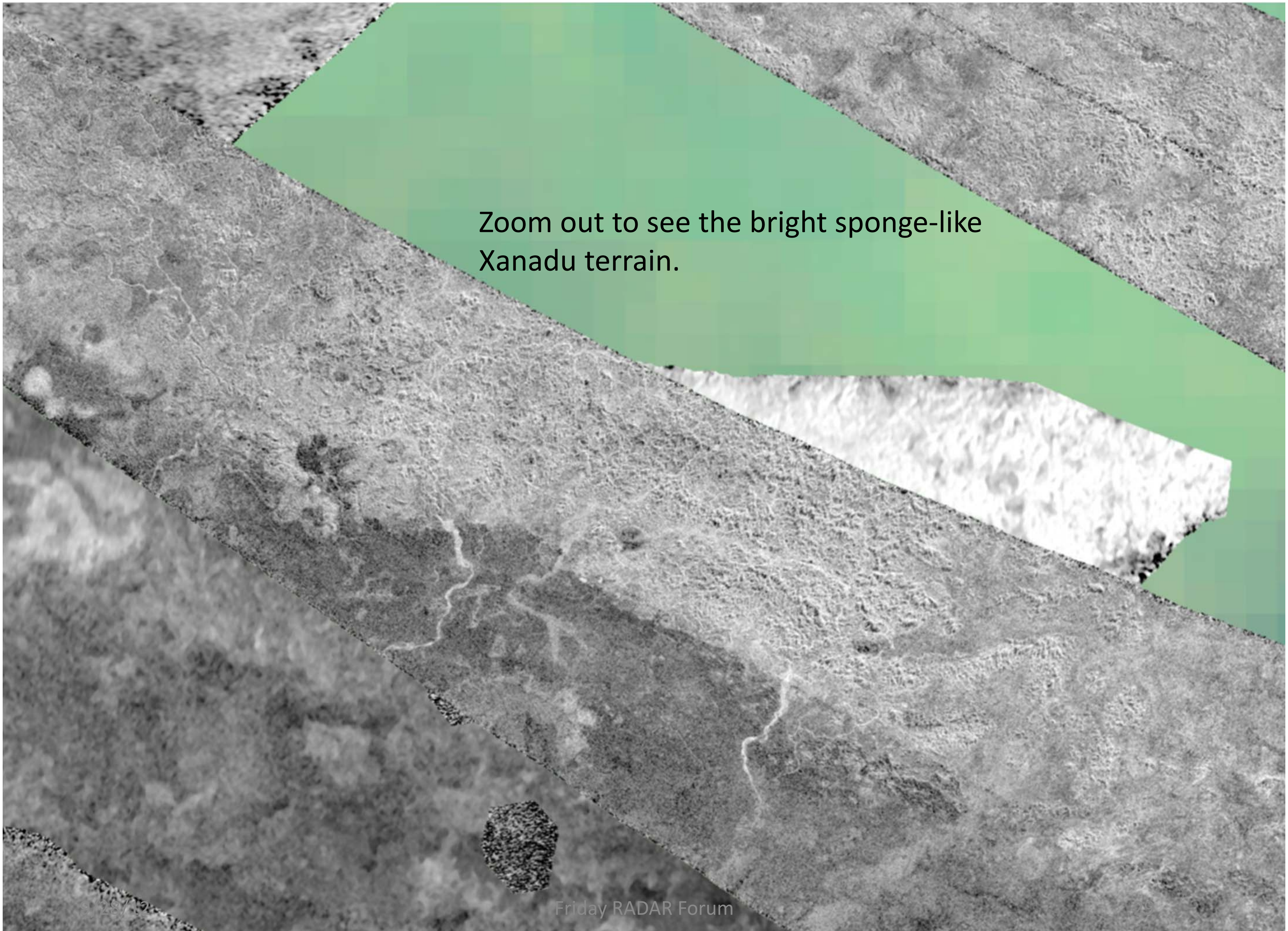
Zoom out to see the bright sponge-like
Xanadu terrain.

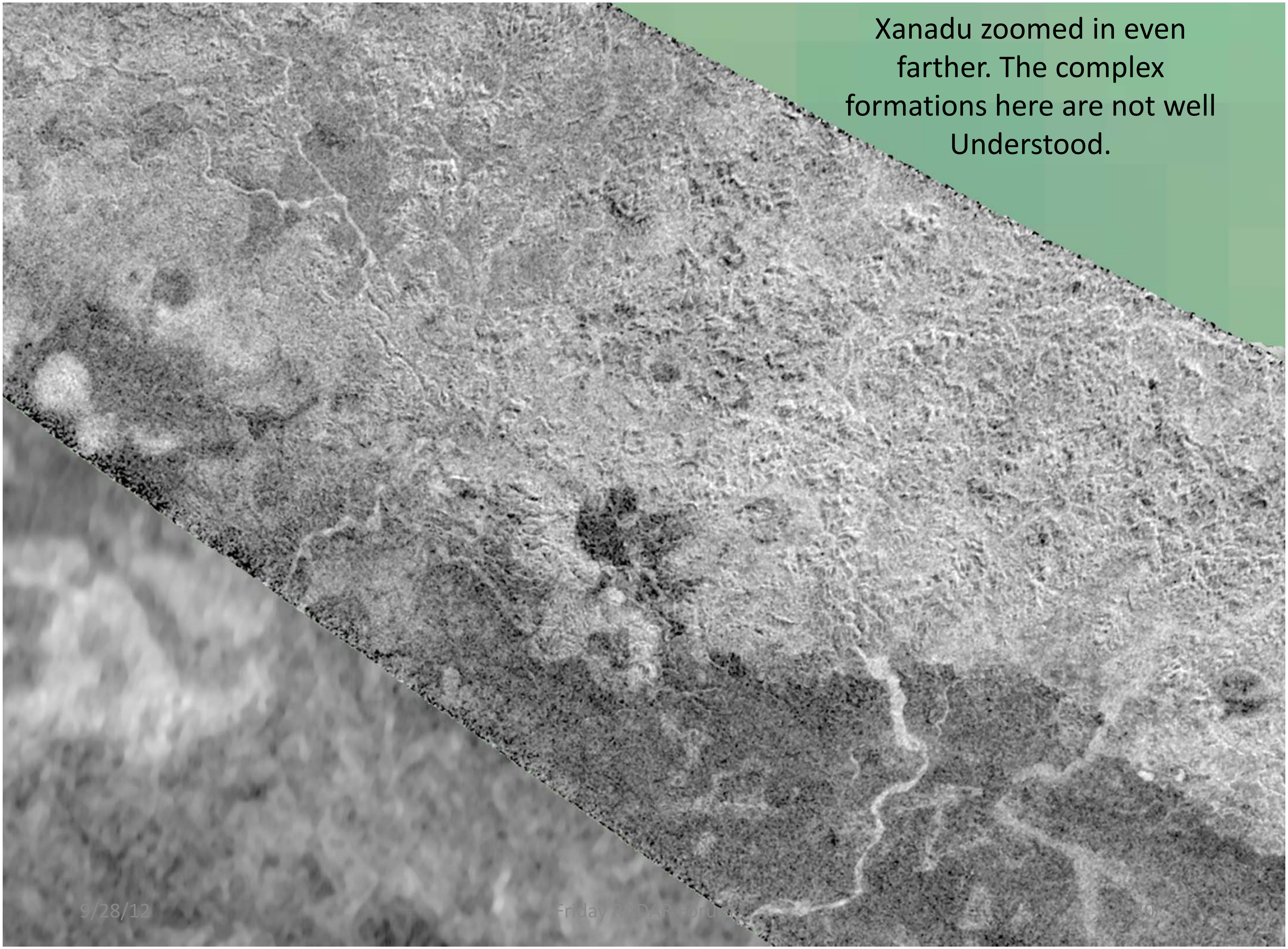

Xanadu zoomed in even farther. The complex formations here are not well Understood.

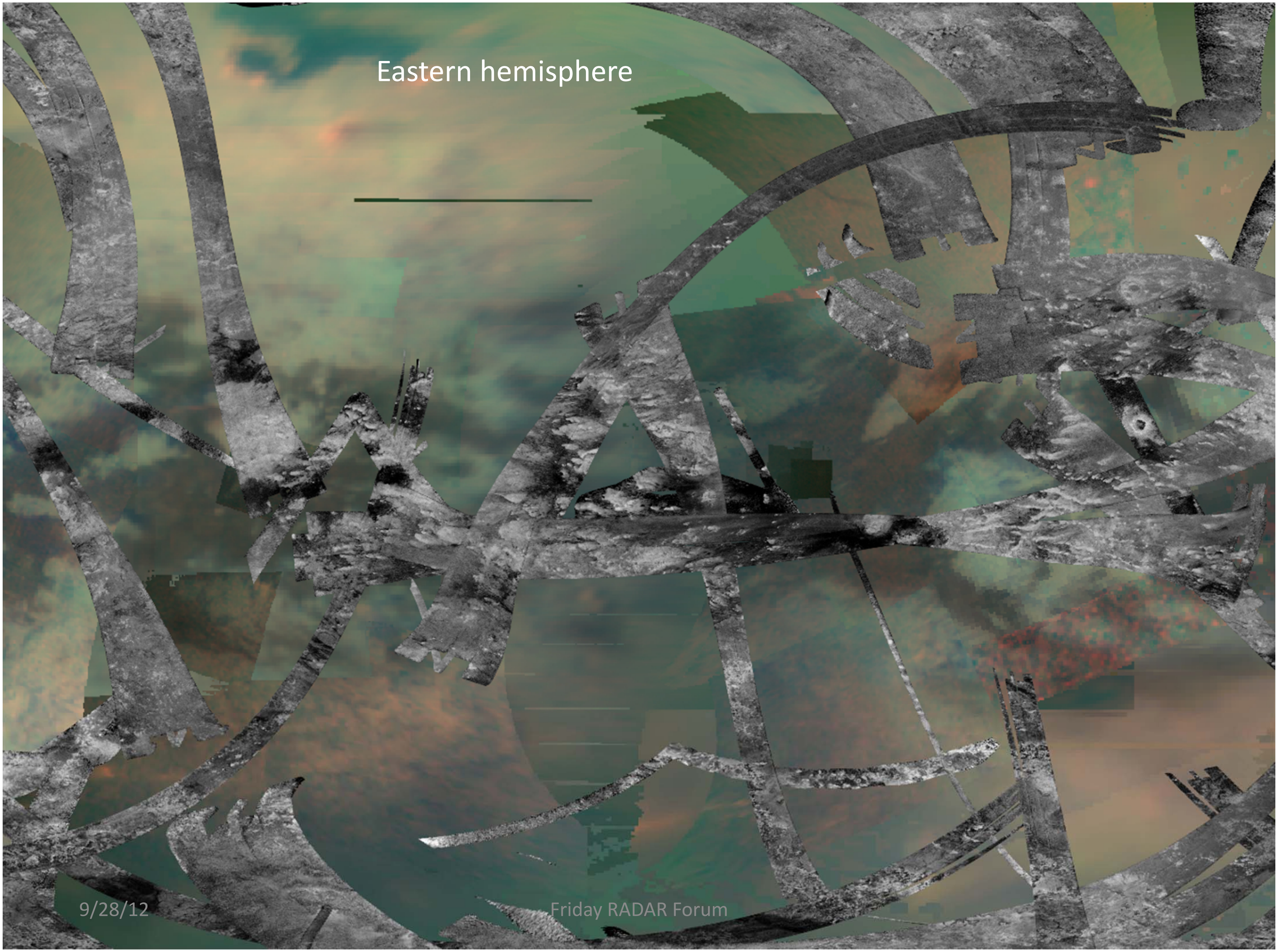
Eastern hemisphere

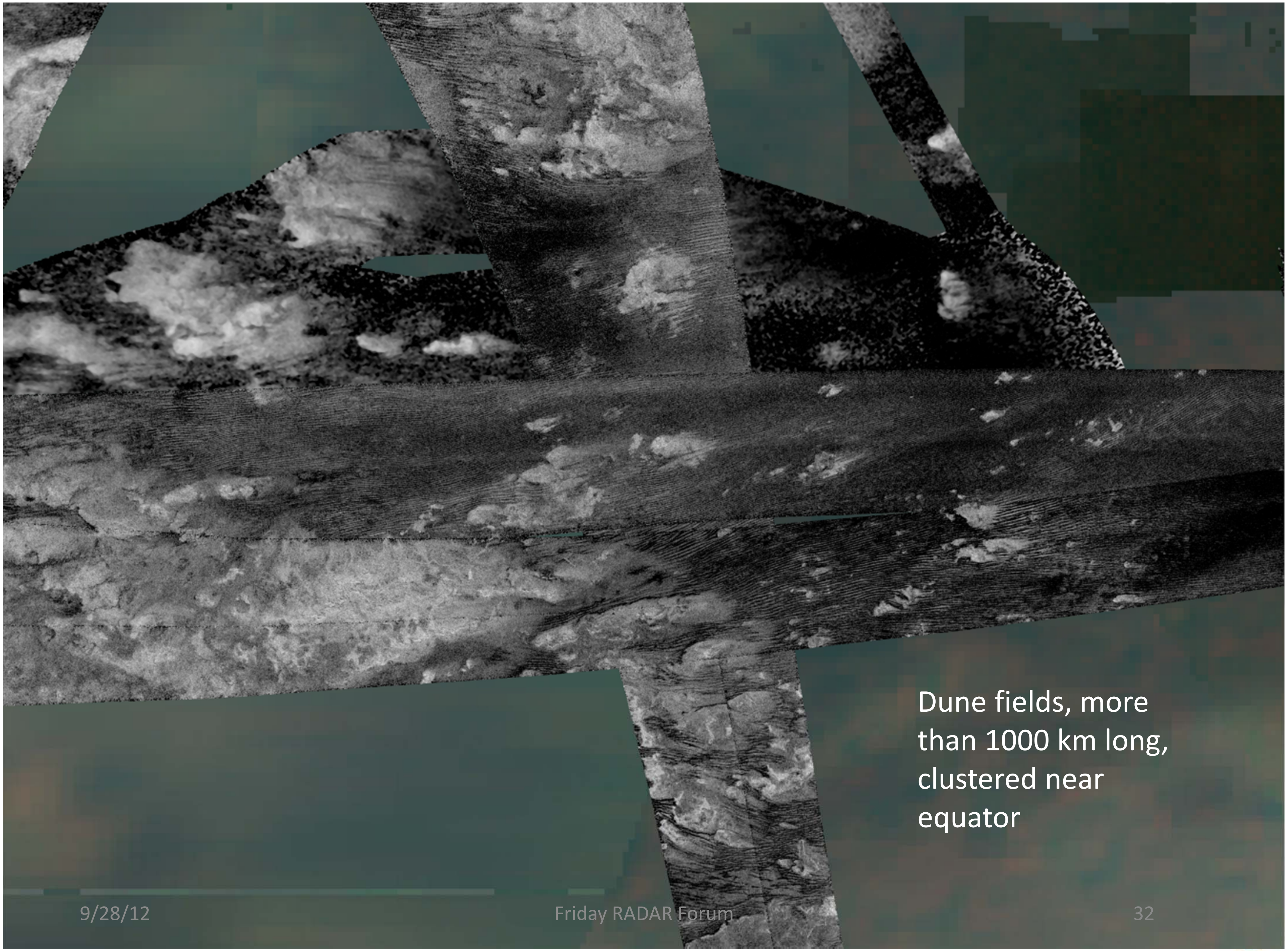

Dune fields, more than 1000 km long, clustered near equator

Close up of Dunes and Bright intrusions

Here radar observation is across the dunes so backscatter do to topography is expected.

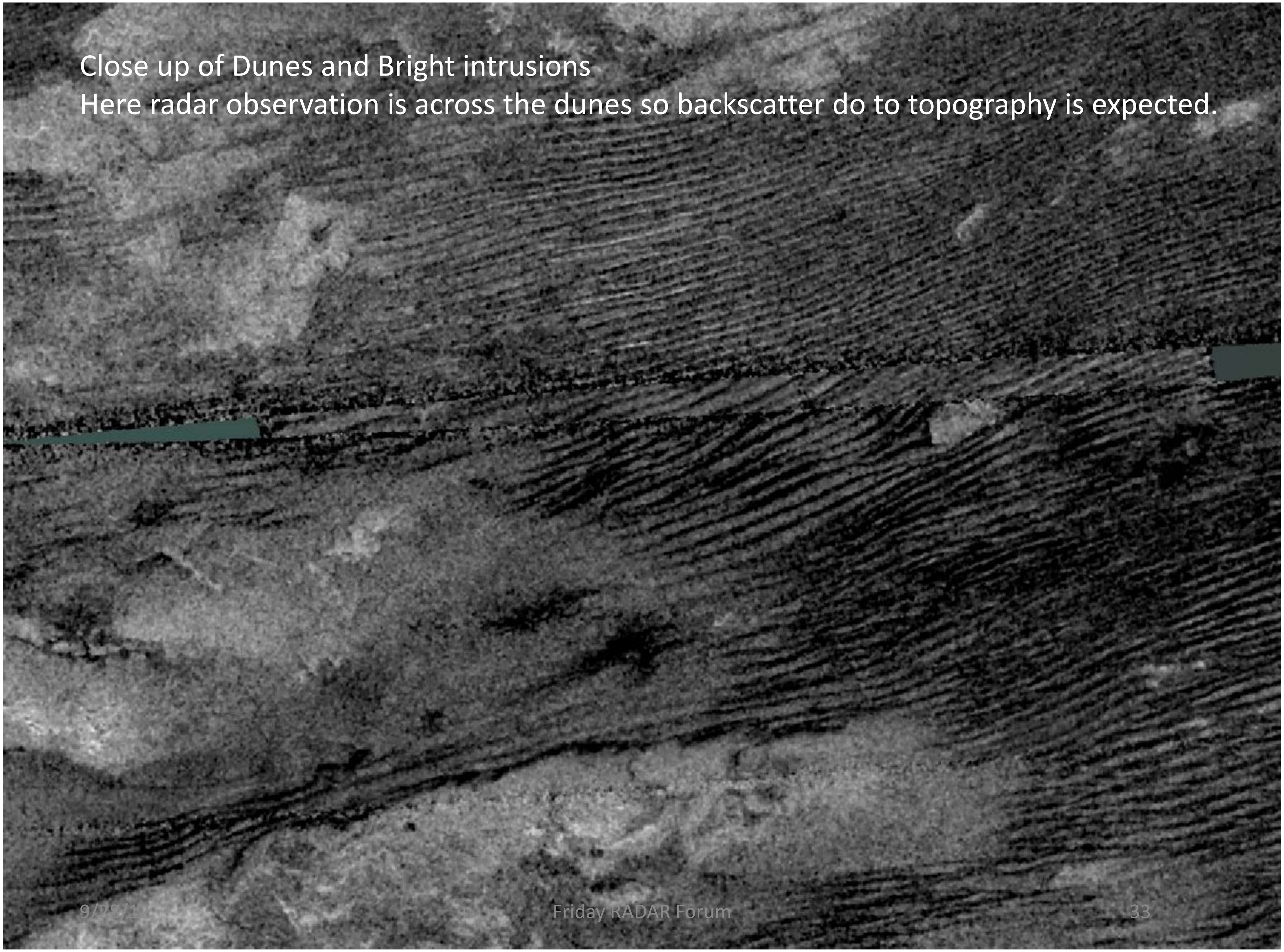

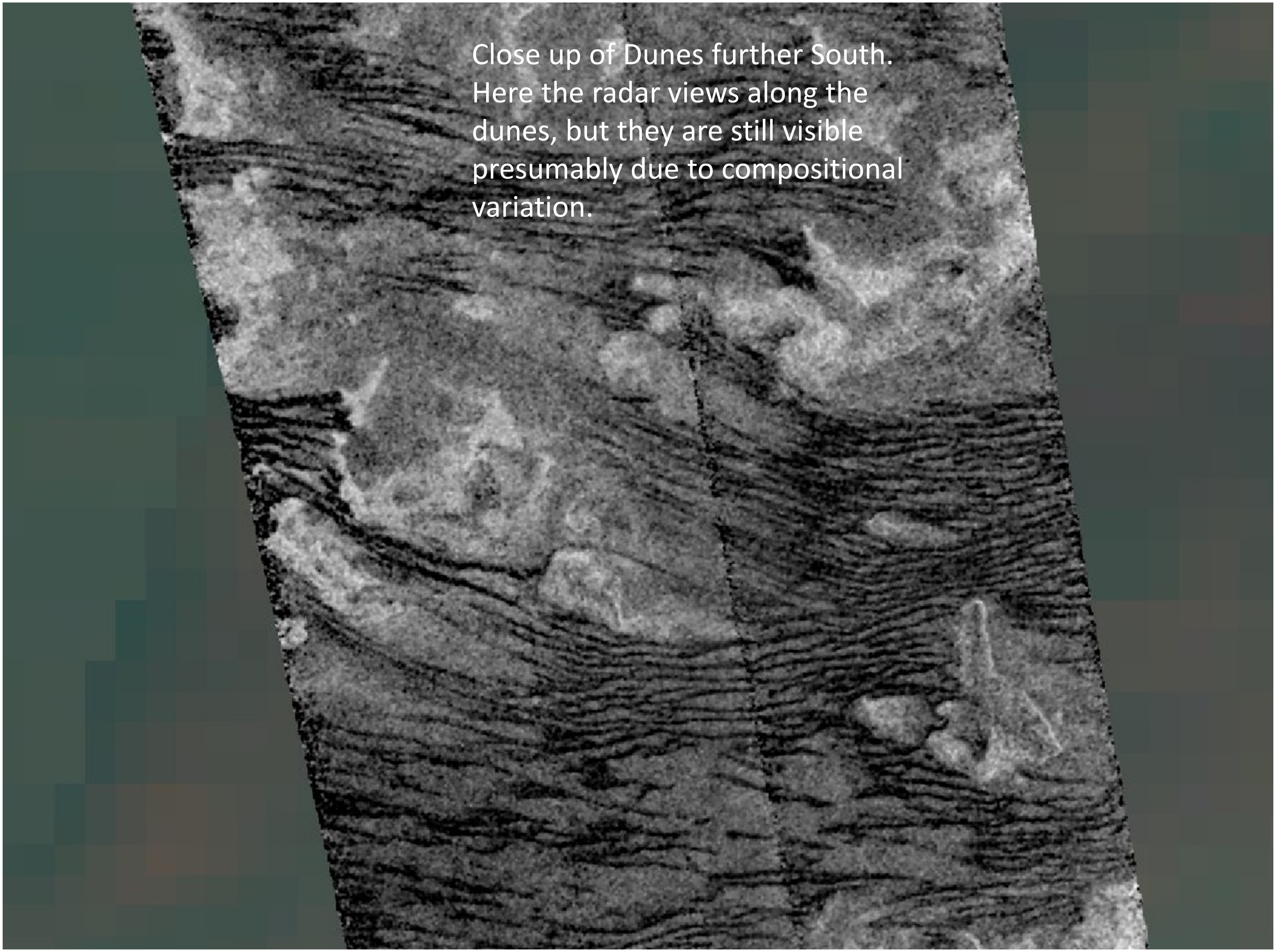
Close up of Dunes further South.
Here the radar views along the dunes, but they are still visible presumably due to compositional variation.

South polar region. Methane lakes are sparser than in the North. Large “river valleys”.

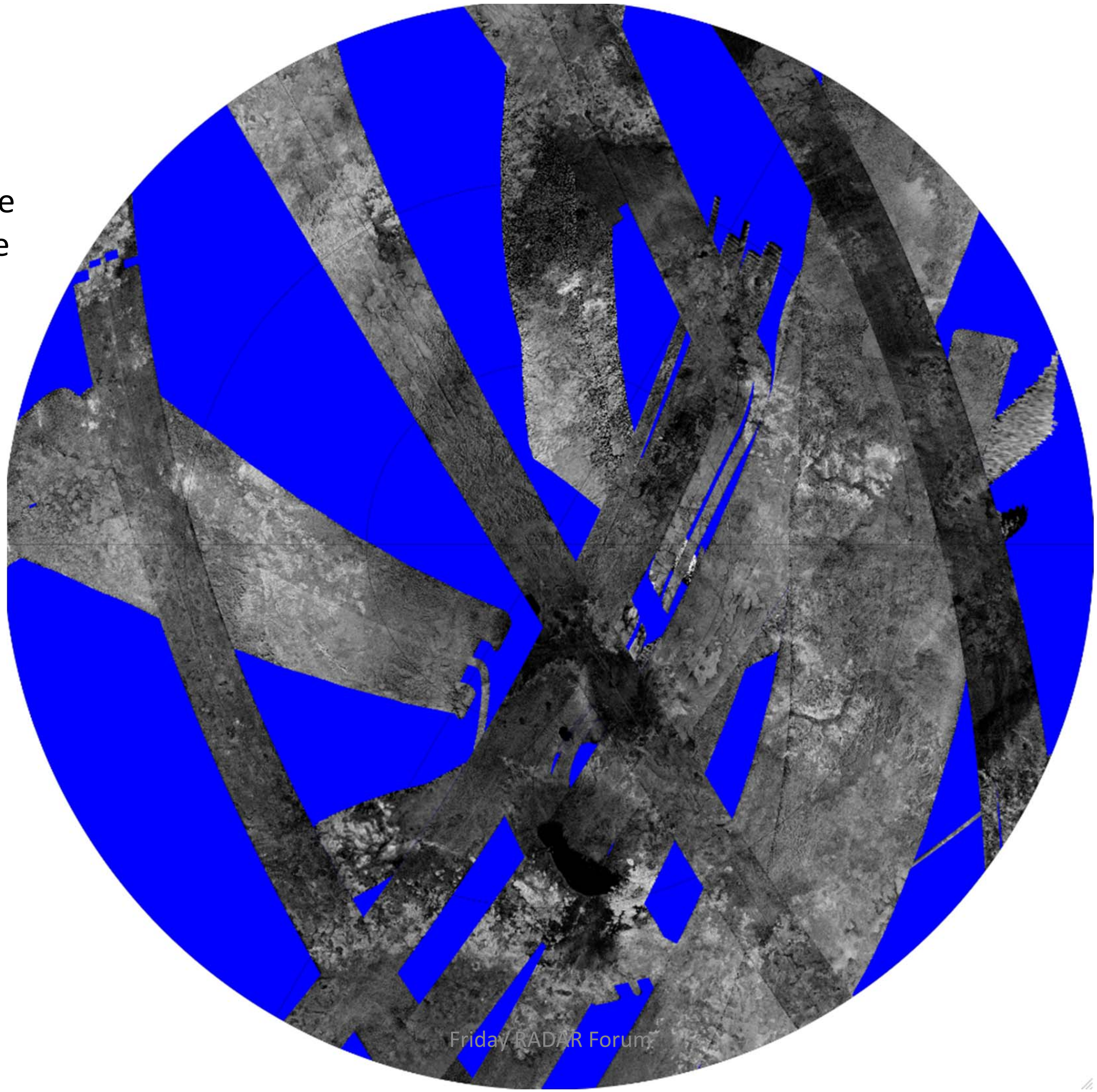

Ontario Lacus, Largest Southern lake

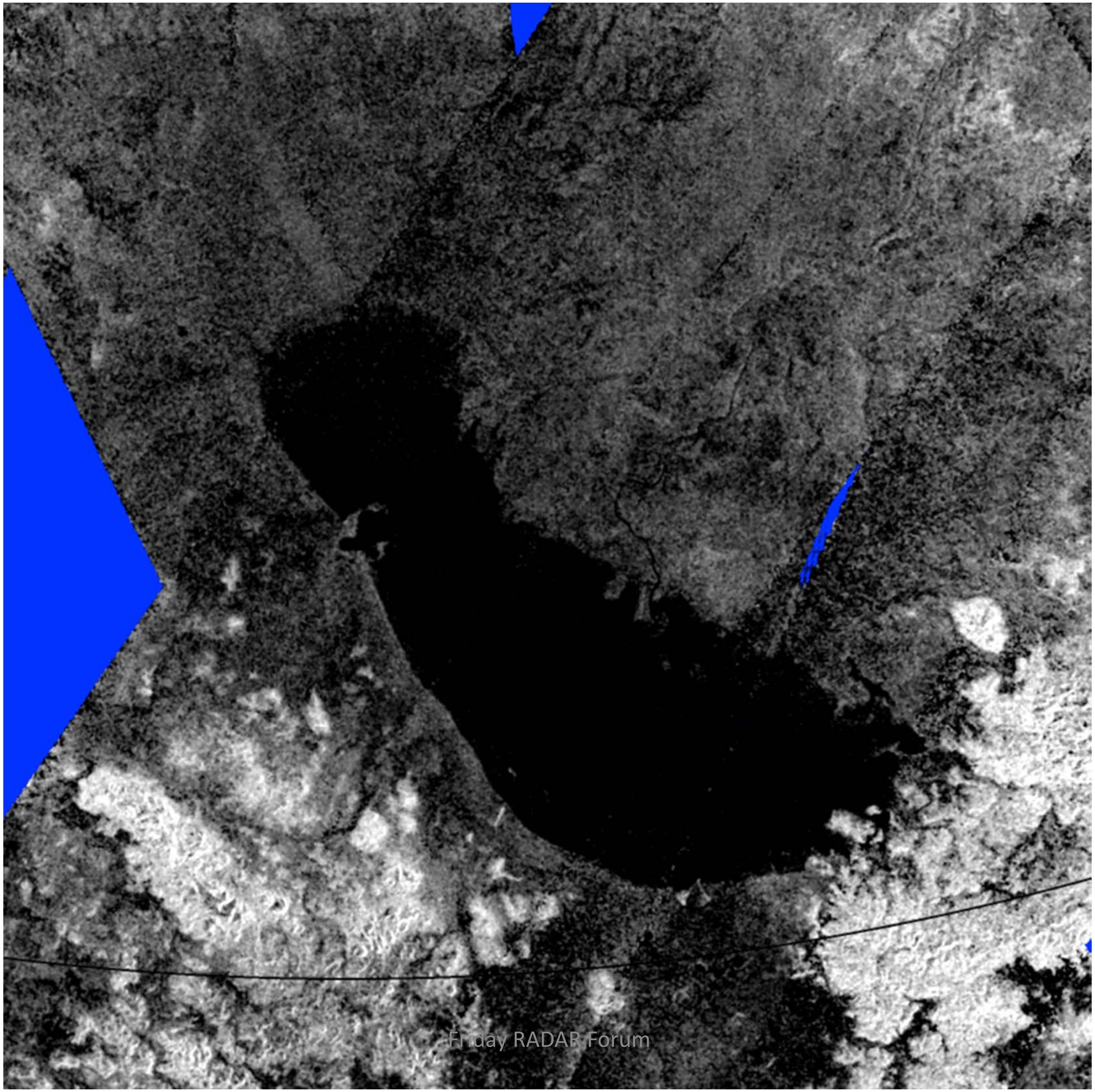

Close up of River Valley

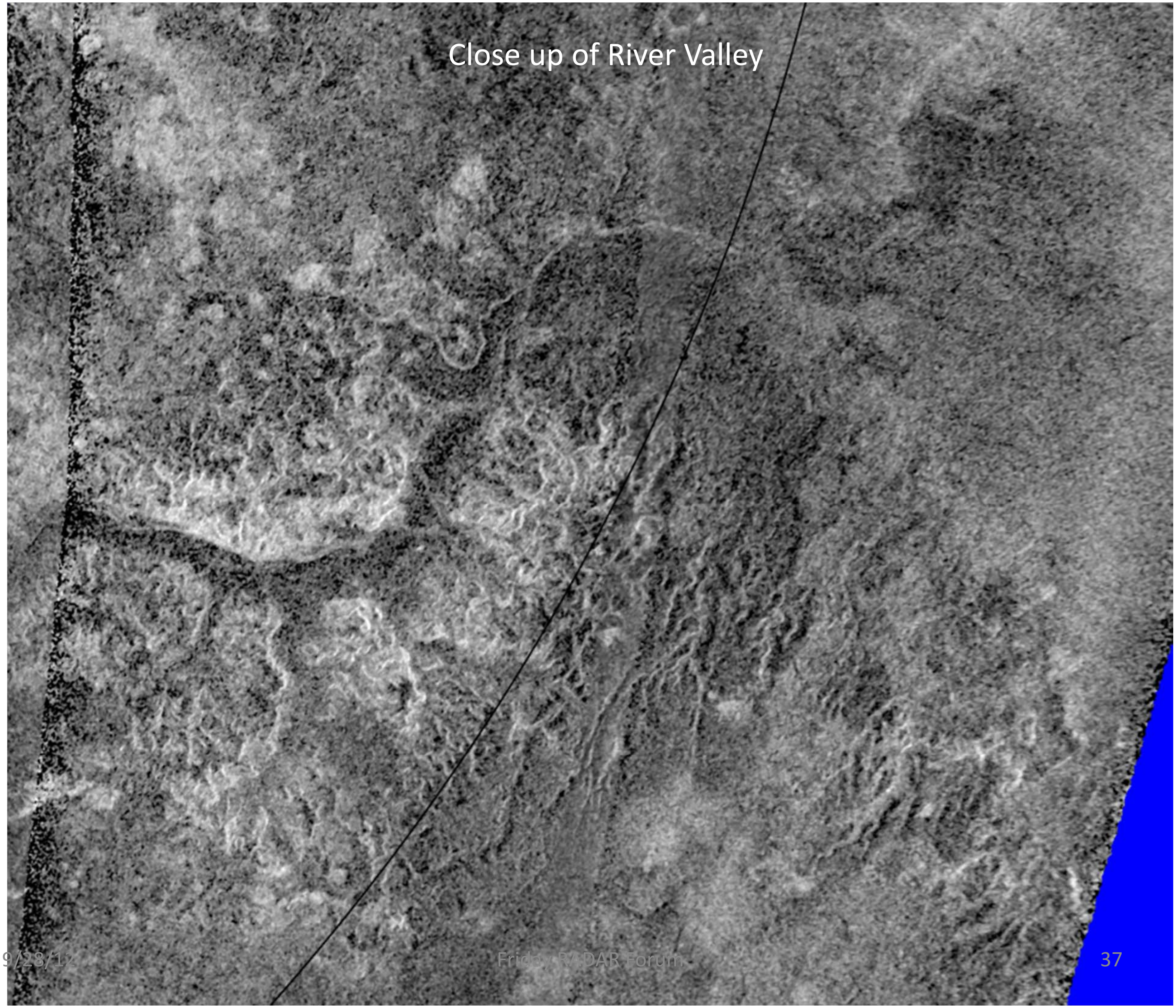

Topography from SAR (SARTopo)

Overview

SAR Pixels are located by range and Doppler values.
For each pixel: Δheight → Δangle → Δgain

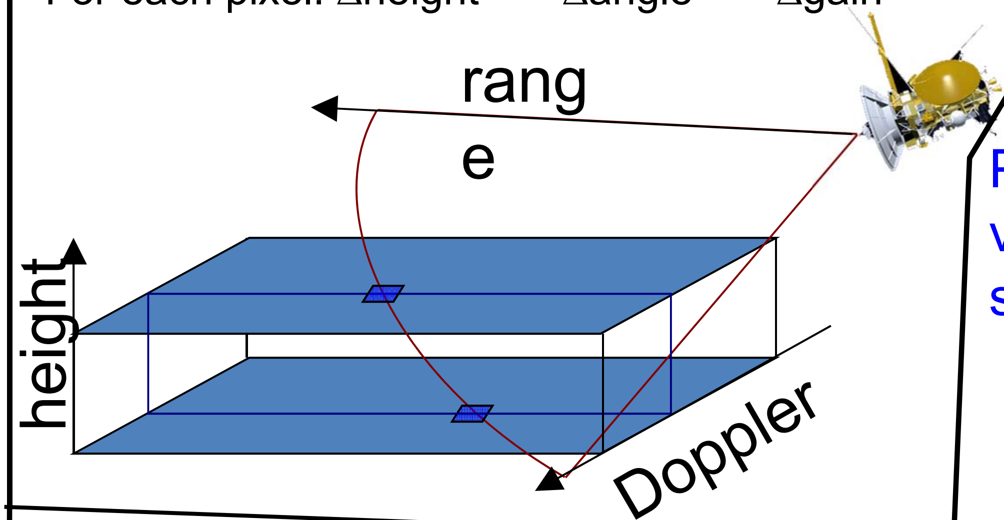

For a uniform scene, the height h maximizes the correlation of P(r) and G(r,h) over range, r.

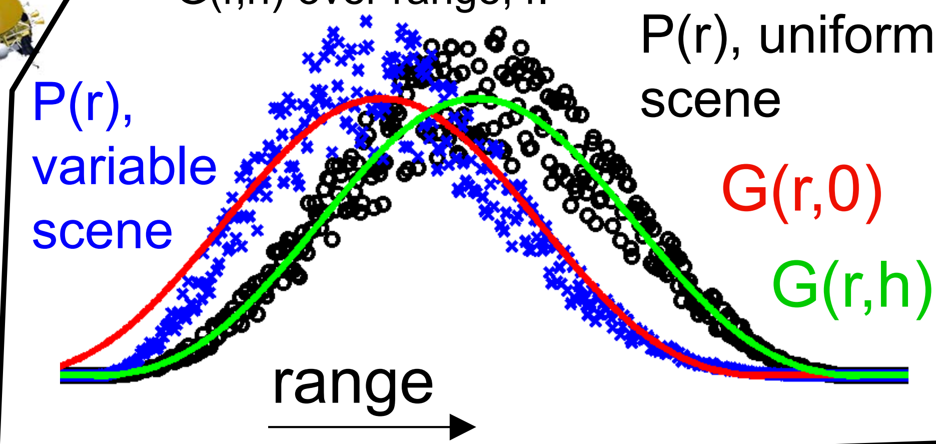

To avoid the variable scene problem,we combine gains and powers from multiple antenna beams: $G_T = (G_1-G_2)/(G_1+G_2)$, $P_T =(P_1-P_2)/(P_1+P_2)$

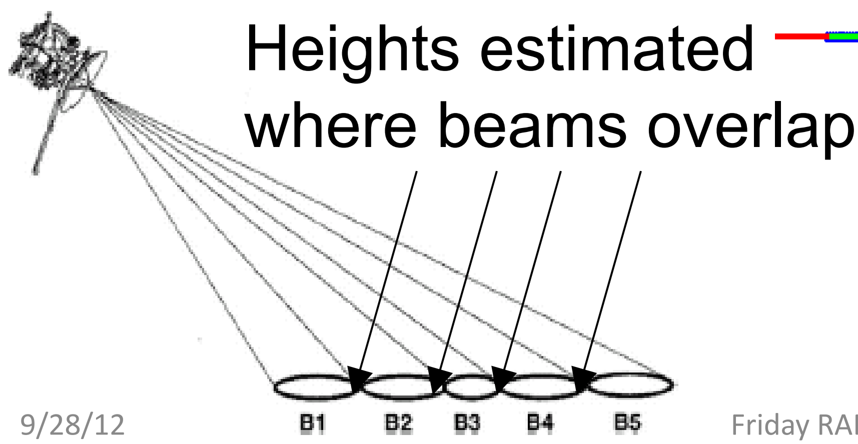

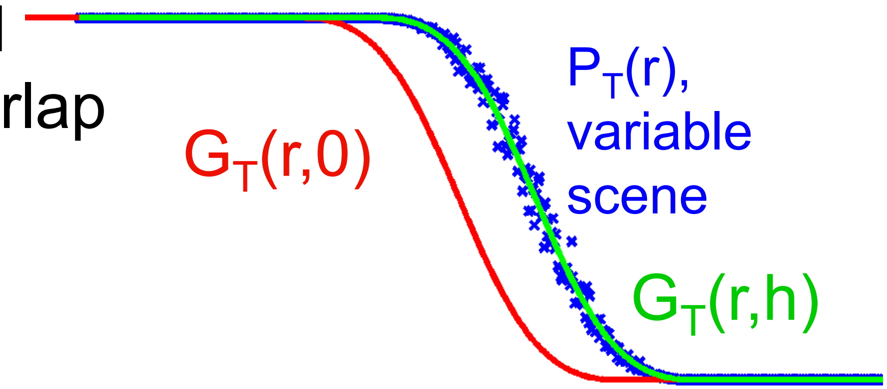

Overview

Beam Mask

2 3 4 5

Processed with h= -500 m

Processed with h= 0 m

Processed with h= +500 m

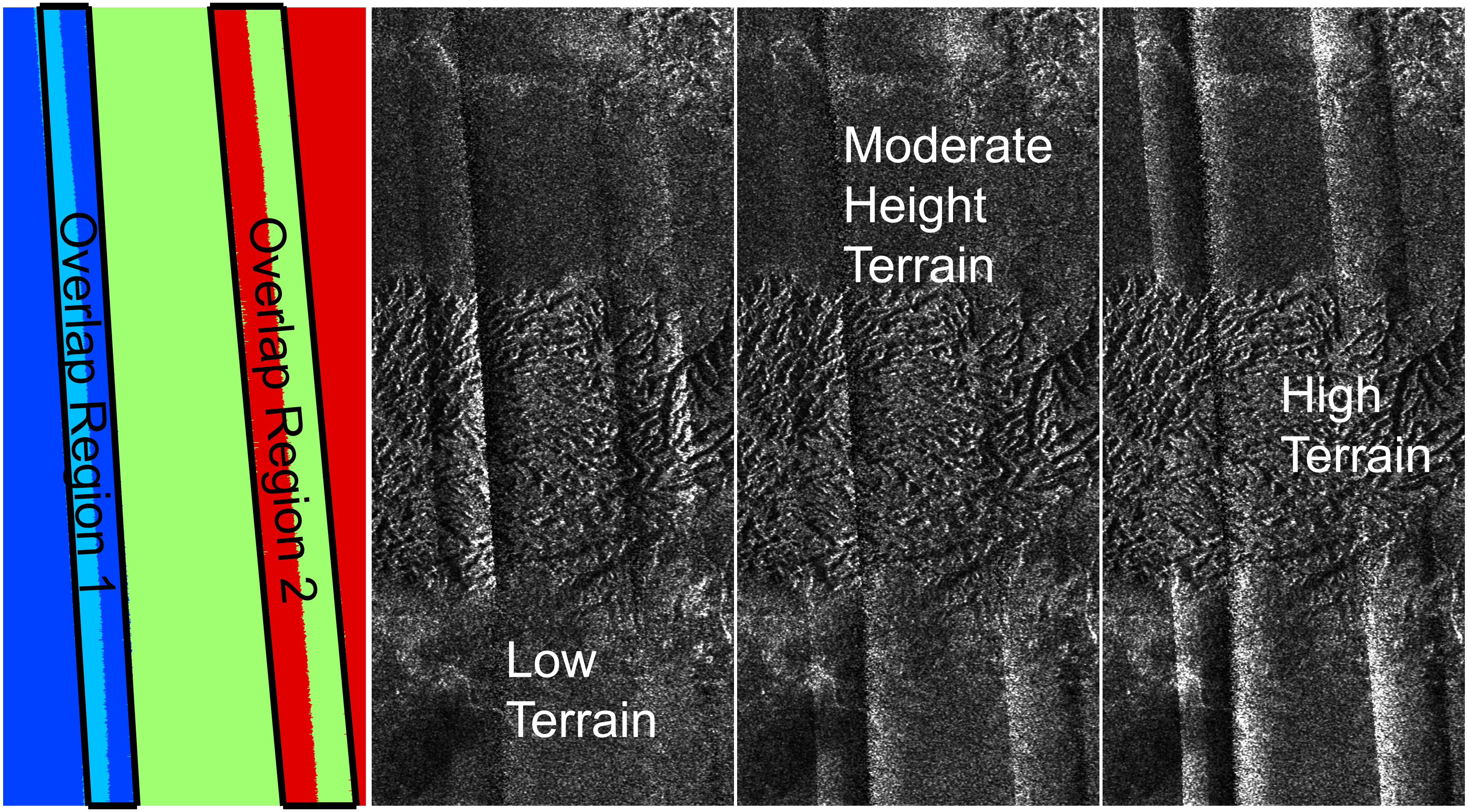

Dark to light band in Overlap Region indicates height underestimation, Light to Dark overestimation. Ignore Banding outside of overlap regions.

Step 1: NRCS Computation

- Normalized Radar Cross-section computed for 17 candidate surface heights from -2 to +2 km.
  - SAR processing used to break up echo power into range and Doppler bins.
  - Power converted to NRCS using radar equation:

$$NRCS = P_{rx} \frac{kr^4}{G^2\left(f_{dop}, r, h\right)A}$$

  - Data geo-located using h=0.
  - Looks from same beam incoherently averaged.
  - Result is NRCS(i,j,b,h) where i,j is surface location, b is beam and h is candidate height.

Step 2: Height Estimation

- Estimate: Beam-to-beam mis-calibration criteria for each candidate height.

$$g(i_0,b,h)=\frac{\sum_{i=i_0}^{i_0+N-1}\sum_{j=j_0}^{j_0+M-1}\sigma_0^b(i,j,h)-\sigma_0^{b+1}(i,j,h)}{\sum_{i=i_0}^{i_0+N-1}\sum_{j=j_0}^{j_0+M-1}\sigma_0^b(i,j,h)+\sigma_0^{b+1}(i,j,h)}$$

- Linearly interpolate to find the height corresponding to the zero crossing.

$$g(i_o,b,h)=\tanh\left(f(i_0,b)\left(h-h_{true}\right)\right)$$

Step 3: Attitude Bias Correction

- Using a network of overlapping SARTopo and nadir altimetry profiles, we estimate and remove height errors due to constant spacecraft attitude knowledge biases for each flyby.

$$\Delta h_f(\mathrm{A}_f, i, b) = \alpha_{fx}\frac{\partial h(i,b)}{\partial \alpha_{fx}} + \alpha_{fy}\frac{\partial h(i,b)}{\partial \alpha_{fy}} + \alpha_{fz}\frac{\partial h(i,b)}{\partial \alpha_{fz}}$$

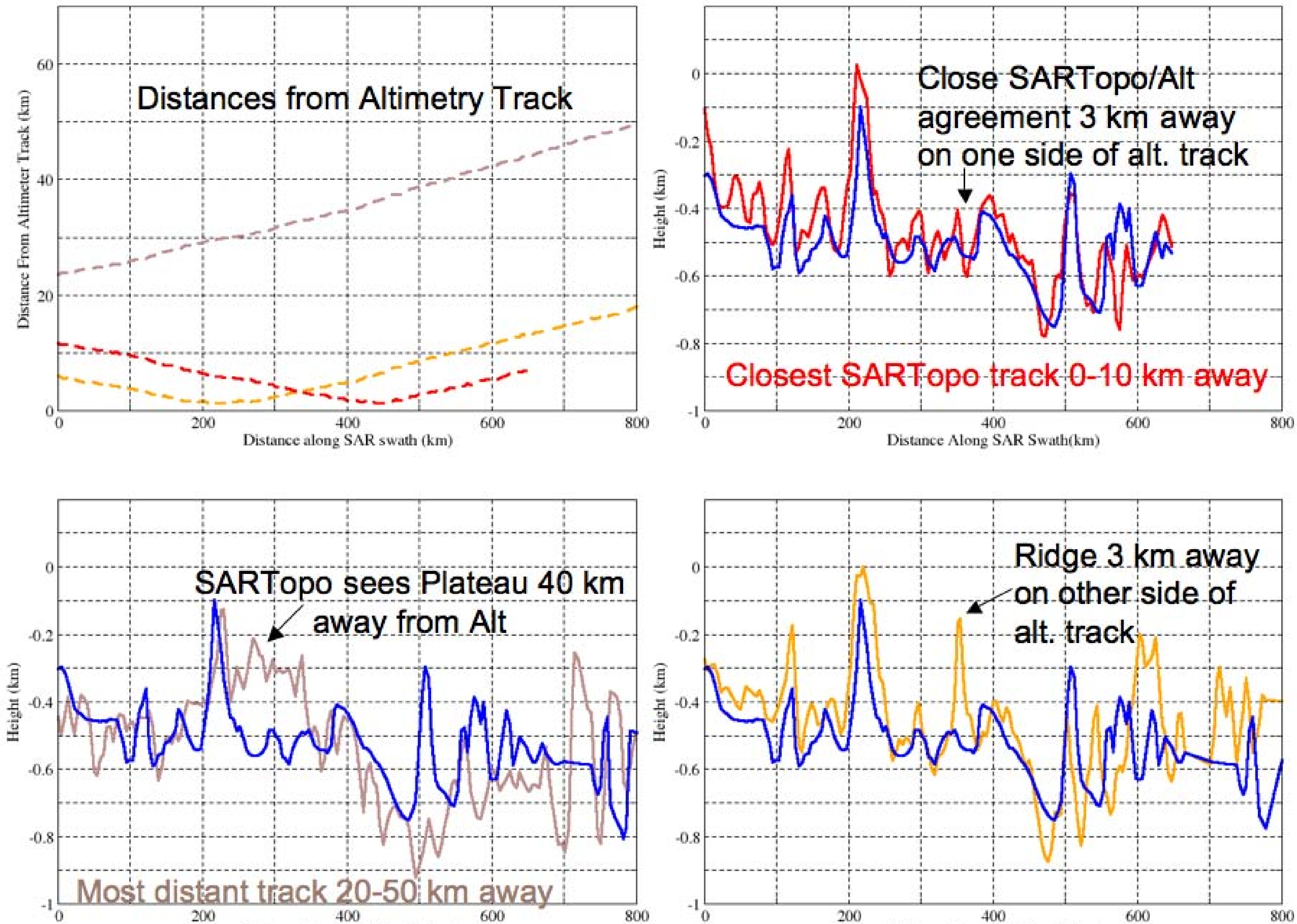
Distances from Altimetry Track
Distance From Altimeter Track (km)
Distance along SAR swath (km)
Close SARTopo/Alt agreement 3 km away on one side of alt. track
Closest SARTopo track 0-10 km away
Height (km)
Distance Along SAR Swath(km)
SARTopo sees Plateau 40 km away from Alt
Most distant track 20-50 km away
Height (km)
Distance Along SAR Swath(km)
Ridge 3 km away on other side of alt. track
Height (km)
Distance Along SAR Swath(km)

North Polar Projection with SARTopo

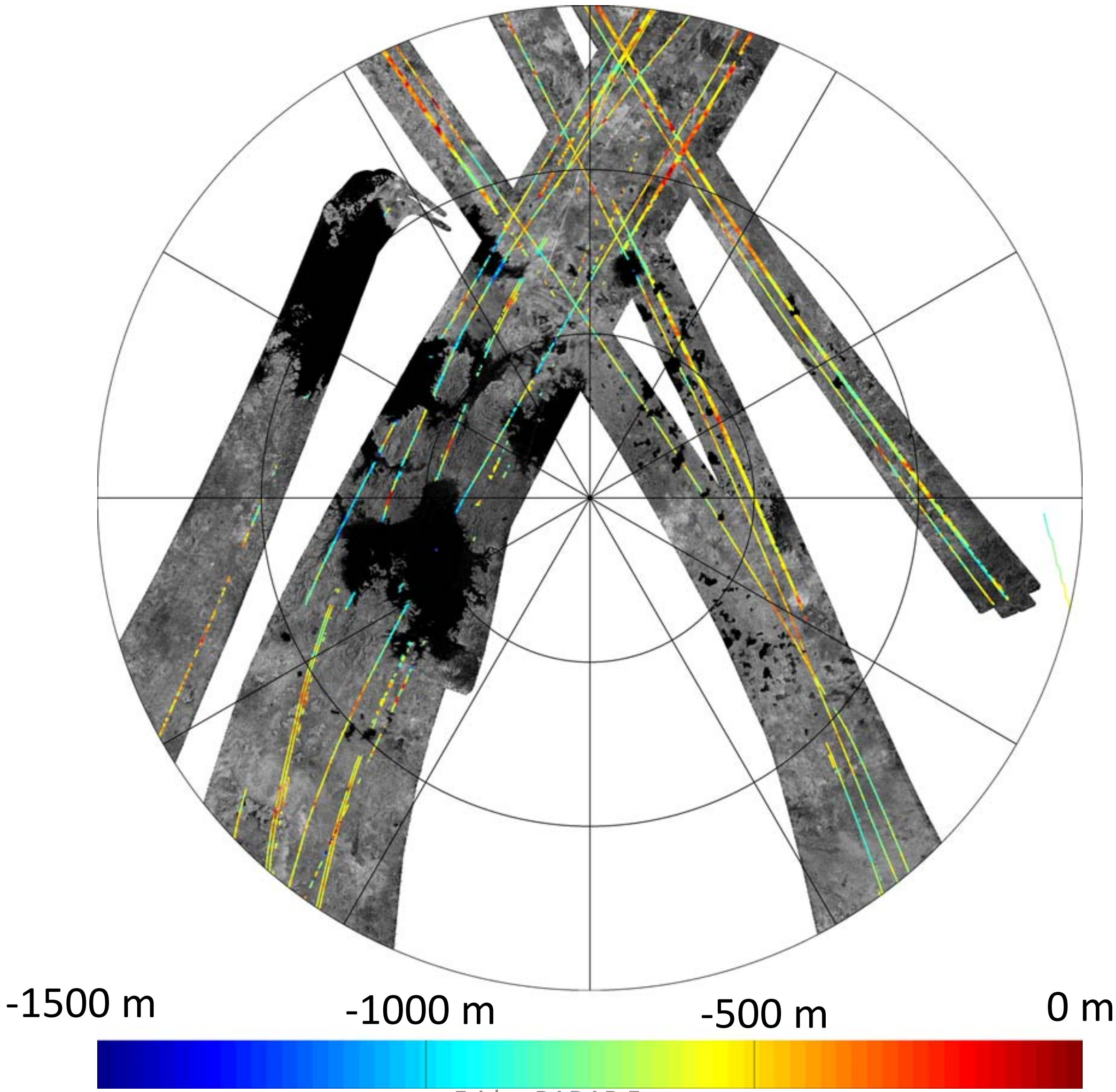

North Polar Projection with SARTopo

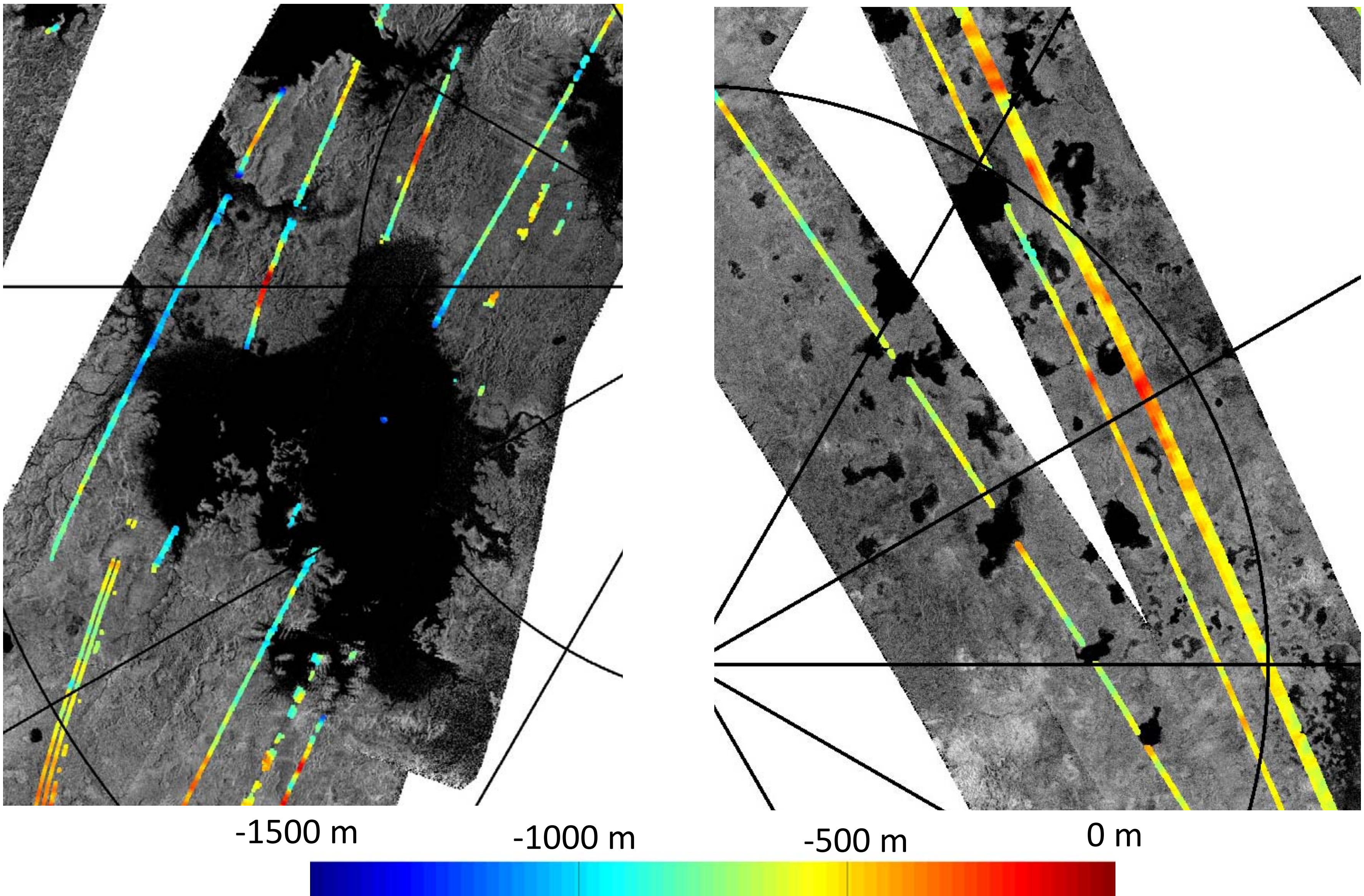

Titan Spin Estimation

Examine Features from Overlapping Scenes

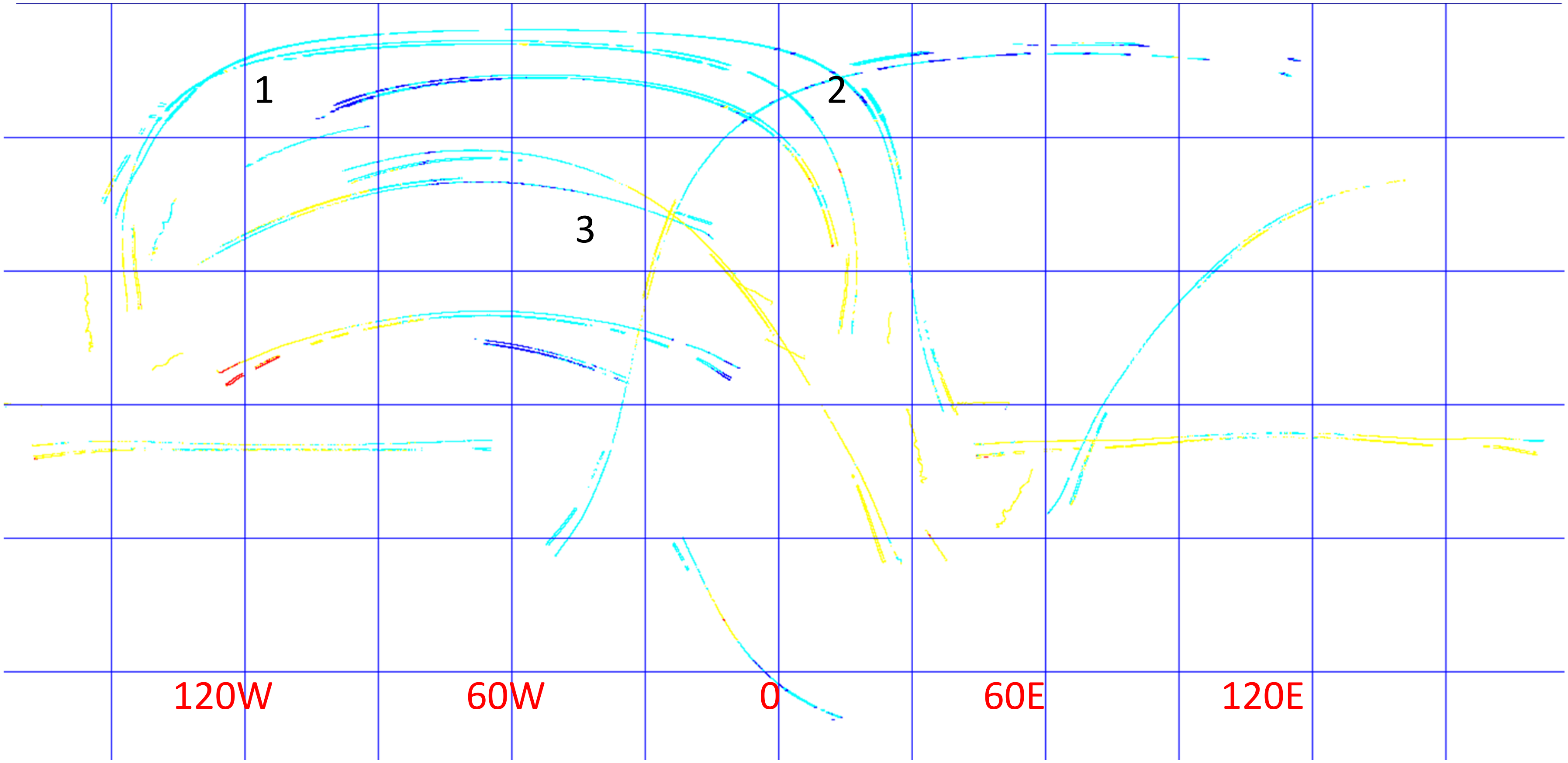

- 17 regions viewed twice by Cassini SAR; 150 identified landmarks.
- Each landmark has two sets of measured Doppler, range, spacecraft position, and spacecraft velocity => Titan body fixed location
- With IAU Titan spin model landmarks are misplaced by 10-30 km.
- We determine a new spin model by minimizing landmark misplacement.

Technique (Slide I)

- Step I: Manually match landmarks between observations.
- Step II: Locate landmarks in inertial frame.
- Step III: Fit spin model to minimize temporal misplacement; 6 parameters are
  - North Pole location (RA, DEC)
  - Spin Rate
  - First order derivatives of Pole location and spin rate w.r.t time

Technique (Slide II)

- 10-30 km observed feature mismatches due to pole location
- 2-3 km mismatches due spin rate and pole wobble

T25

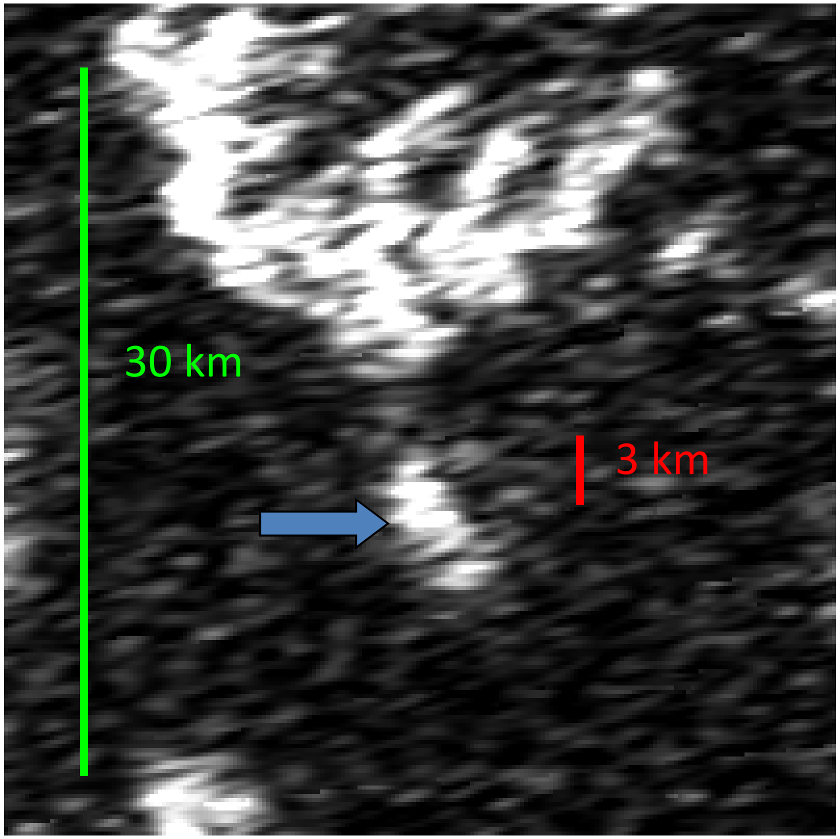

T28

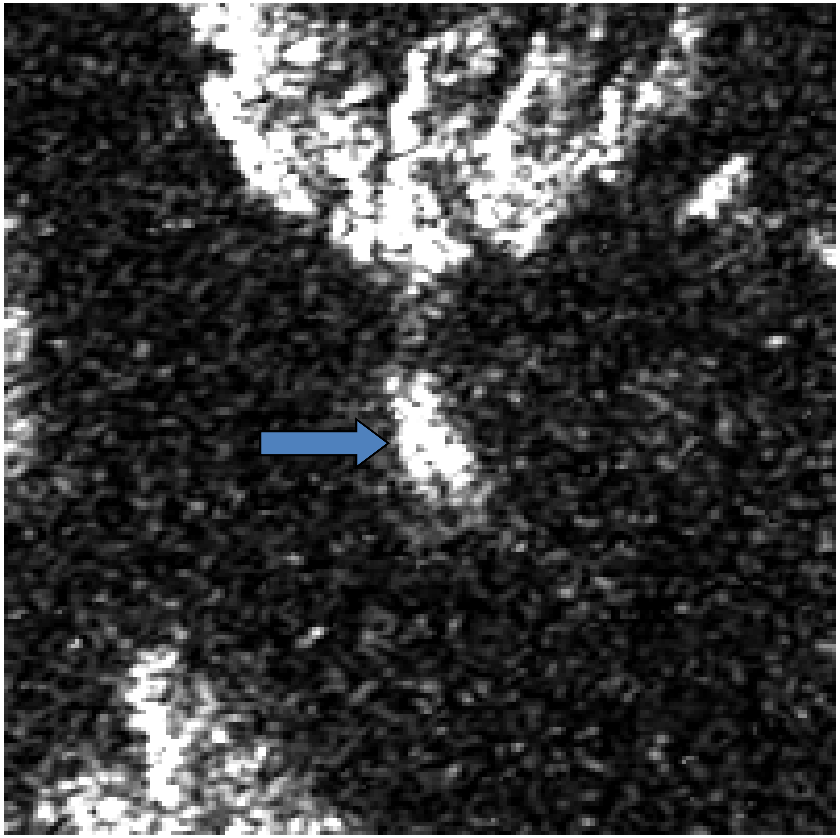

Validation (Slide I)

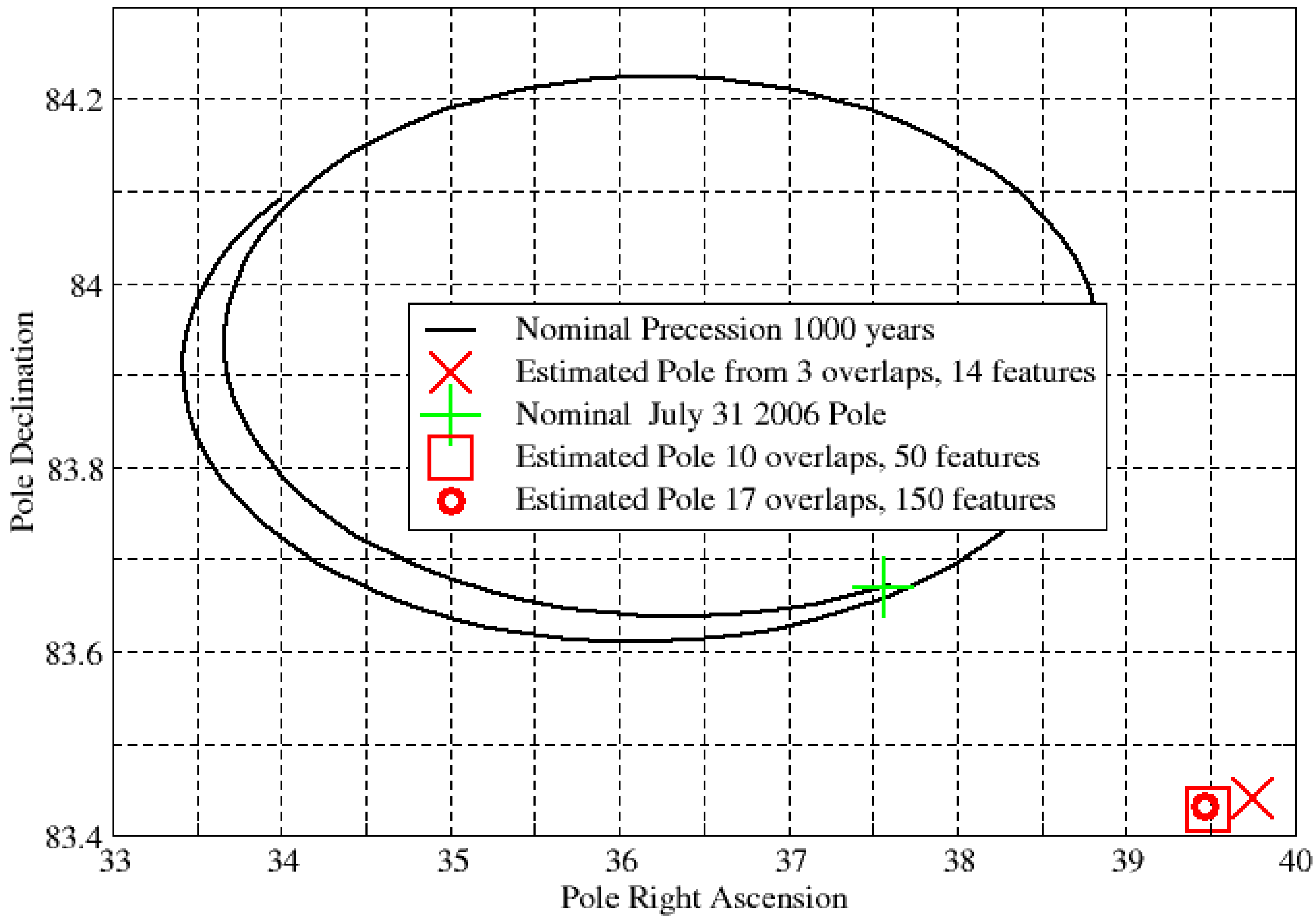

Updates to Spin Parameters

New Periodic Spin Rate Fit

- Pole [RA,DEC]=[39.47,83.44]
  - Obliquity 0.3 degrees
  - Nearly coplanar with orbit normal and Laplacian
- Spin rate (sync+Periodic)
  - 1700 day period
  - 0.00026 deg/day amplitude
- Pole precession rate
  - consistent with precession rate of orbit normal
- Fit residual = 770 m

Previously Published Fit

- Pole [RA,DEC]=[39.48,83.43]
  - Obliquity 0.3 degrees
  - Not coplanar with orbit normal and Laplacian
- Spin rate (linear with t)
  - Sync. + 0.001 deg/day
  - + 0.0005 deg/day/year
- Pole precession rate
  - DEC rate ~ 0
  - RA rate -0.3 deg/year = 15 X orbit normal RA rate
- Fit residual 1300 m

Best Periodic Spin Rate Fit

Residual errors in km in surface coordinates are
LON ERR = 550 m RMS, LAT ERR = 550 m RMS.

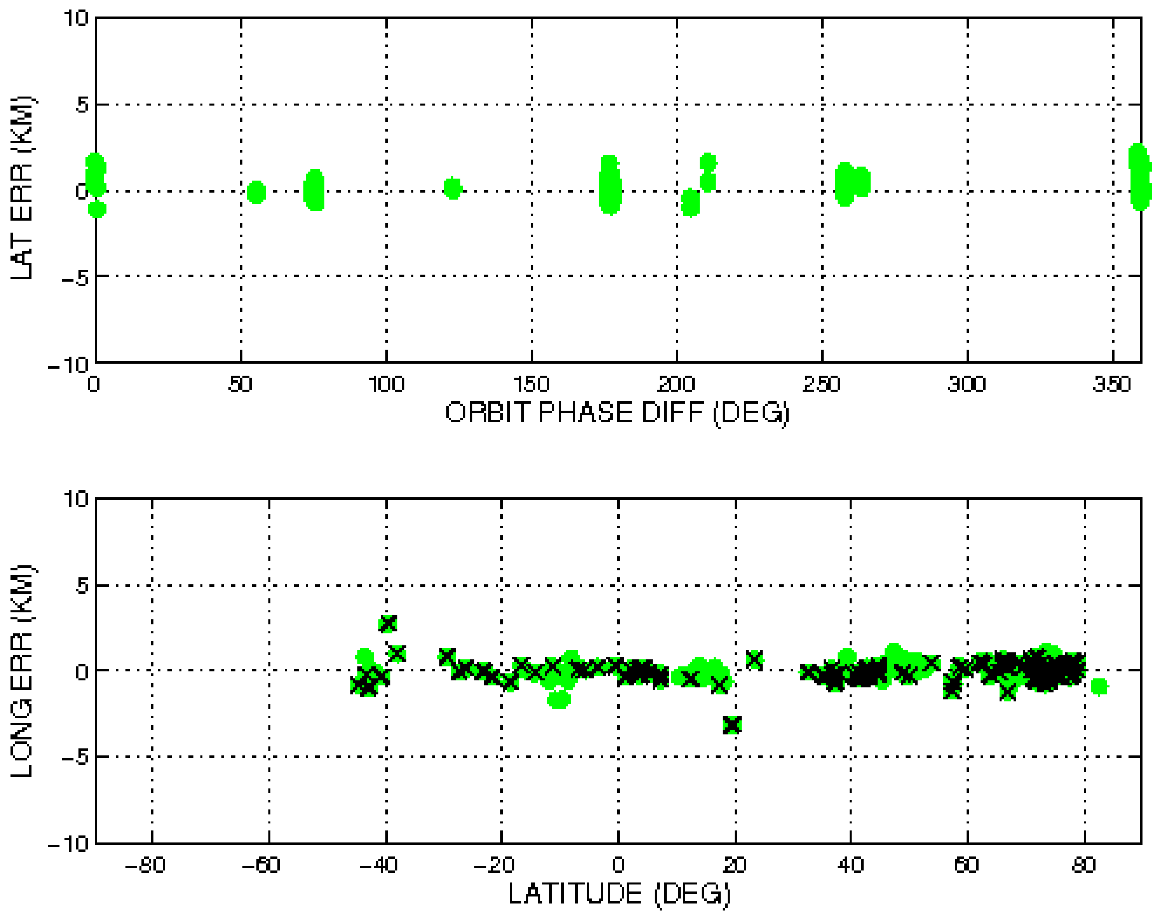

Constant Pole, Synchronous Fit

LATERR RMS is 650 m.
LONERR RMS is 1790 m
Largest errors (3-6 km) for near equatorial tiepoints observed more than 6 months apart. (X's are observed within 6 months)

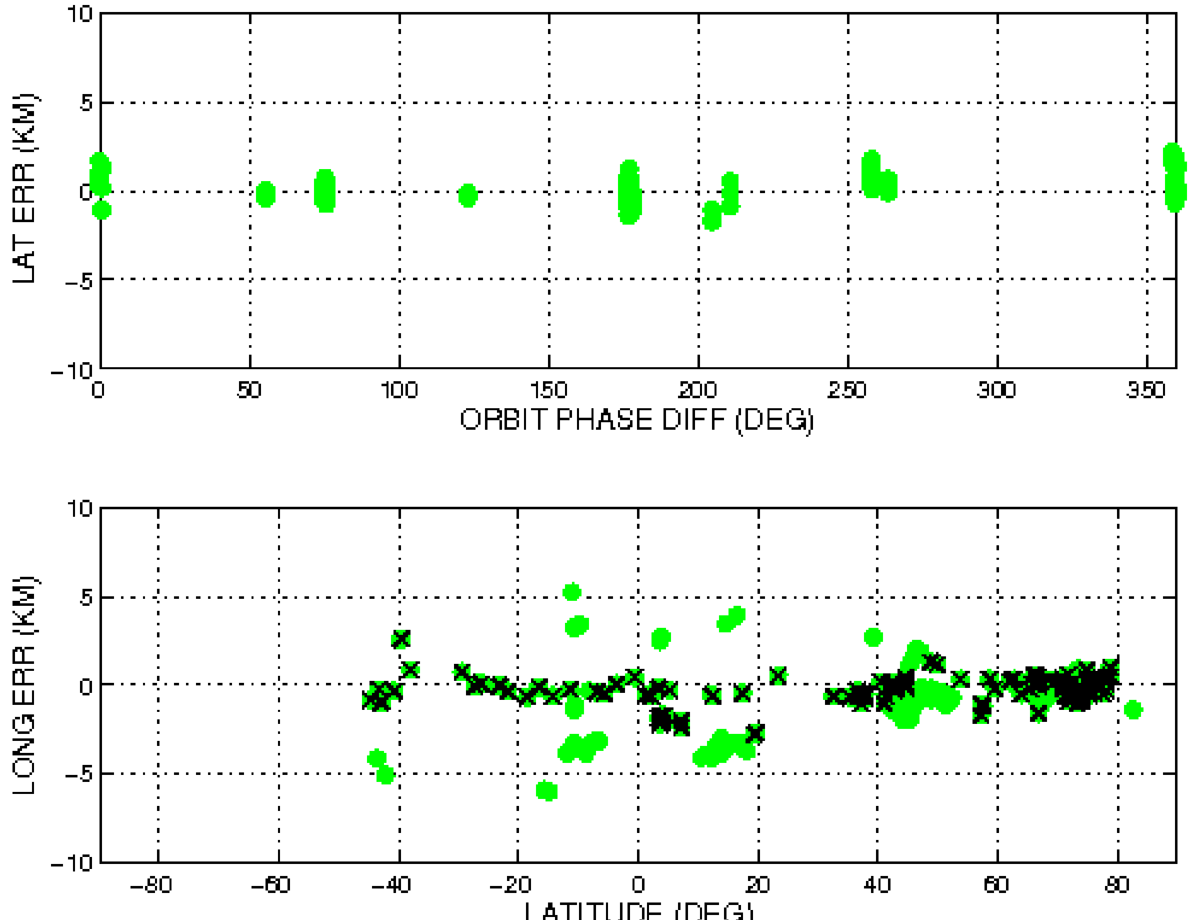

Longitudinal Displacement vs. Delta time for synchronous fit

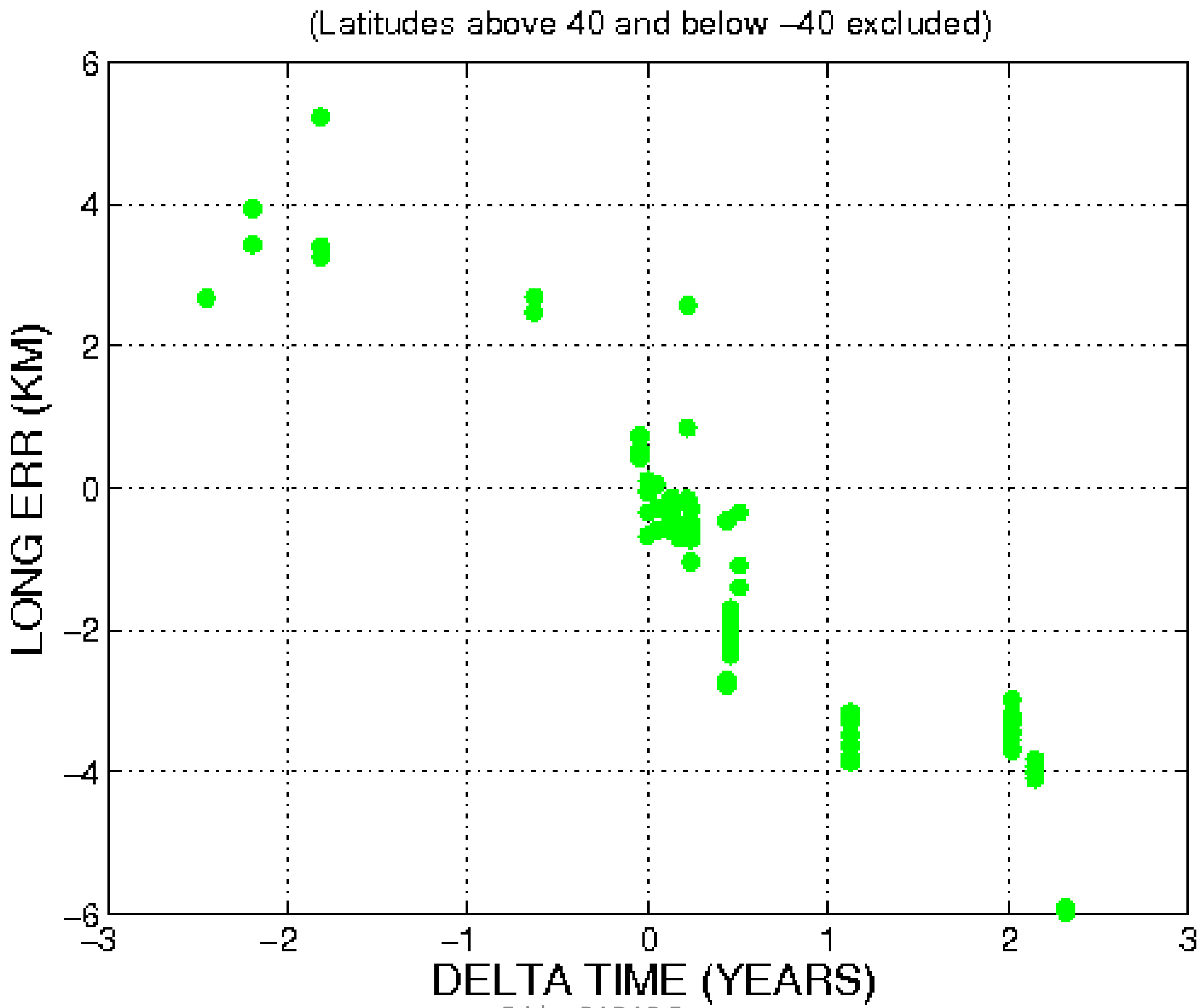

Best Periodic Spin Rate (Period =1700 days)

No residual longitudinal biases as a function of time between tiepoint observations.

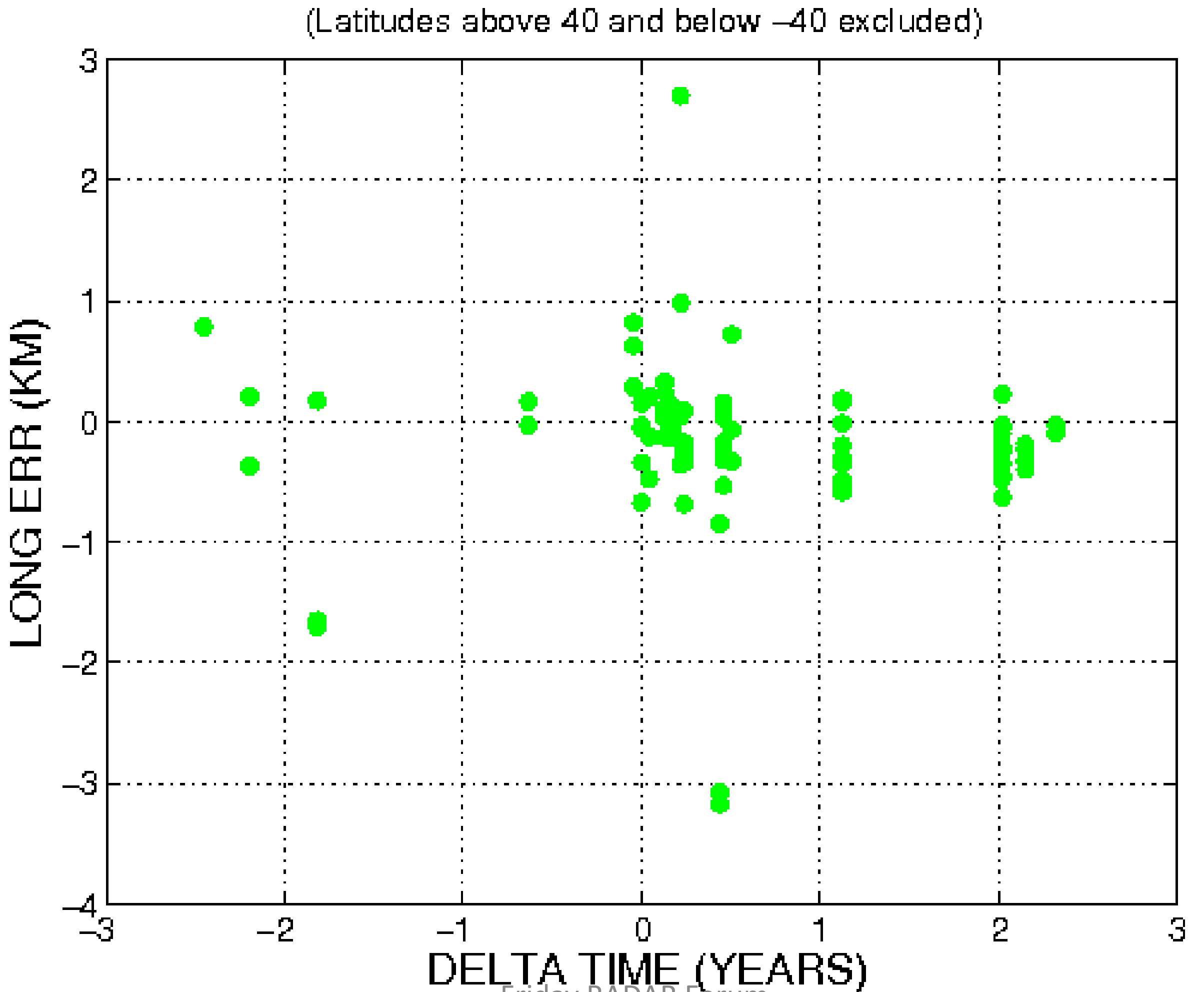

Best fit for Spin Rate Period= Saturn orbit

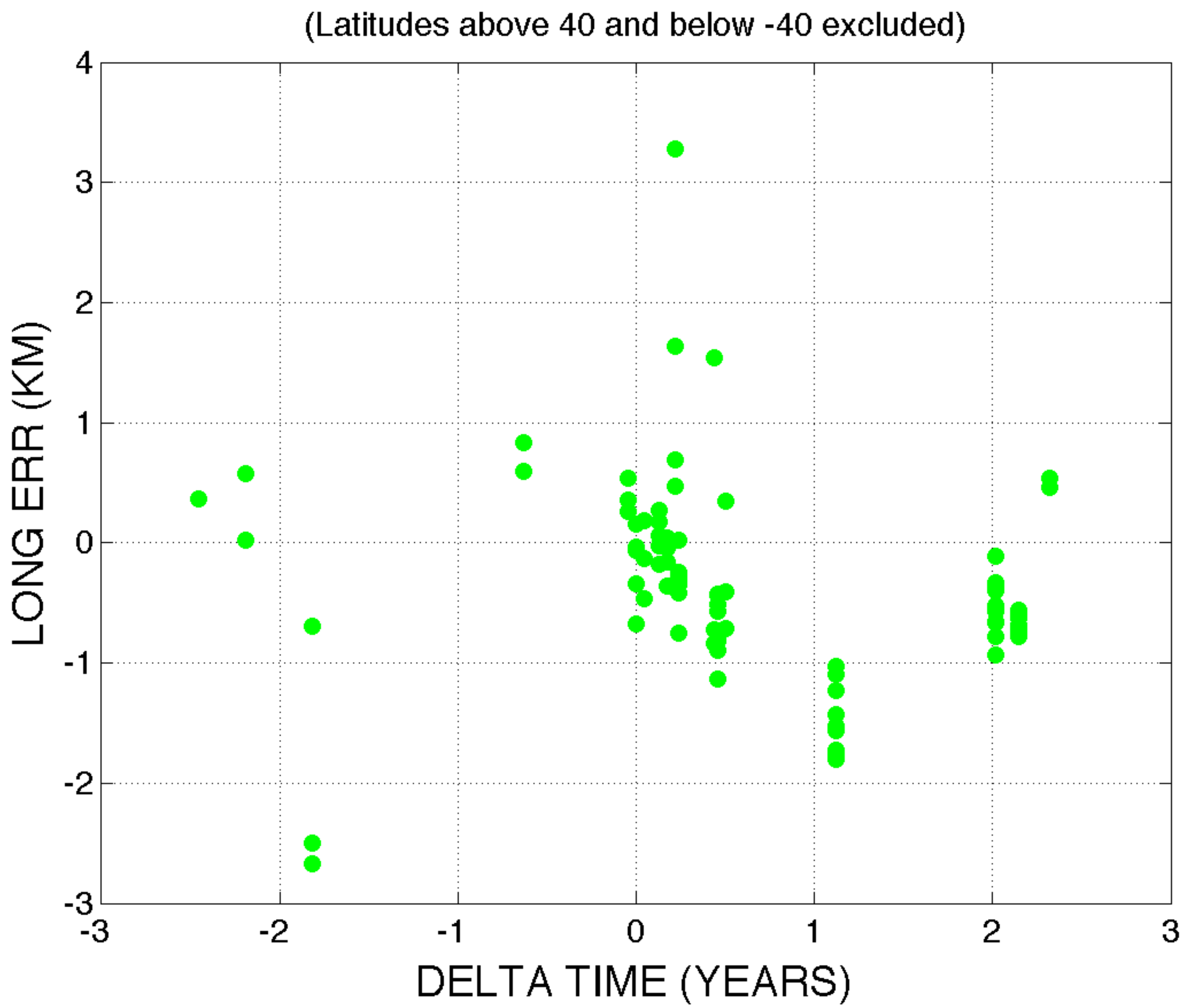

Summary

- Cassini RADAR has discovered numerous surface features on Titan that were previously unknown, including liquid methane seas, river valleys, and equatorial dunes.
- Topographical data from SAR has determined that Titan is oblate, more so than one would expect from independently obtained models of Titan's geoid.
- The spin axis of Titan has a larger obliquity 0.3 degrees than one would expect (0.1) from assuming a rigid body with its determined moment of Inertia.
  - This may indicate an internal ocean.

Related Papers

- Ralph D. Lorenz , Elizabeth P. Turtle, Bryan Stiles, Alice Le Gall, Alexander Hayes, Oded Aharonson, Charles A. Wood, Ellen Stofan, and Randy Kirk, **"Hyposometry Of Titan,"** Icarus, Volume 211, No. 1, pp. 699-706. 2011.
- Giuseppe Mitri, Michael T. Bland, Adam P. Showman, Jani Radebaugh, Bryan Stiles, Rosaly M. C. Lopes, Jonathan I. Lunine, and Robert T. Pappalardo, **"Mountains On Titan: Modeling And Observations,"** Journal Of Geophysical Research, Vol. 115, E10002. 2011.
- Bryan W. Stiles, Scott Hensley, Yonggyu Gim, David M. Bates, et al., **"Determining Titan surface topography from Cassini SAR Data,"** Icarus, Vol. 202, No.2, pp. 584-598. 2009.
- Howard Zebker, Bryan W. Stiles, Scott Hensley, Ralph D. Lorenz, and Randolph L. Kirk, **"Size and Shape of Saturn's Moon Titan from Cassini Radar Altimeter and SAR Monopulse Observations,"** Science, Vol. 324 no. 5929, pp. 921-923. 2009.
- Bryan W. Stiles, Randolph L. Kirk, Ralph D. Lorenz, Scott Hensley, et al., **"Determining Titan's Spin State from Cassini RADAR Images,"** The Astronomical Journal, Vol 135 No 5, pp. 1669-1680. 2008.
- Stofan E.R., C. Elachi, J.I. Lunine, R.D. Lorenz, B. Stiles, et al, **"The lakes of Titan,"** Nature 445, pp. 61-64. 2007.
- C. Elachi, S. Wall, M. Allison,Y. Anderson, R. Boehmer, P. Callahan, P. Encrenaz, E. Flamini, G. Francescetti, Y. Gim, G. Hamilton, S. Hensley, M. Janssen, W. Johnson, K. Kelleher, R. Kirk, R. Lopes, R. Lorenz, J. Lunine, D. Muhleman, S. Ostro, F. Paganelli, G. Picardi, F. Posa, L. Roth, R. Seu, S. Shaffer, L. Soderblom, B. Stiles, E. Stofan, S. Vetrella, R. West, C. Wood, L. Wye, and H. Zebker, **"Cassini Radar Views the Surface of Titan,"** Science, Vol. 308, No. 5724, pp. 970-974. 2005.